Lappeenrannan teknillinen yliopisto
Lappeenranta University of Technology

Heikki Kurttila

Isentropic Exergy and Pressure of the Shock Wave Caused by the Explosion of a Pressure Vessel

Thesis for the degree of Doctor of Science (Technology) to be presented with due permission for public examination and criticism in the auditorium of the Student House at Lappeenranta University of Technology, Lappeenranta, on the 14th of November, 2003, at noon.

Acta Universitatis
Lappeenrantaensis
164

Supervisor	Professor Pertti Sarkomaa Department of Energy Technology Lappeenranta University of Tecnology Finland
Reviewers	Doctor Matti Harkoma Finnish Defence Forces Technical Research Centre Finland
	Doctor Mikko Vuoristo Nexplo Vihtavuori Oy Finland
Opponents	Docent Timo Talonpoika Alstom Finland Oy Finland
	Doctor Mikko Vuoristo

ISBN 951-764-813-8
ISBN 951-764-819-7 (PDF)
ISSN 1456-4491
Lappeenrannan teknillinen yliopisto
Digipaino 2003

Abstract

Heikki Kurttila

Isentropic Exergy and Pressure of the Shock Wave Caused by the Explosion of a Pressure Vessel

Lappeenranta, 2003
Acta Universitatis Lappeenrantaensis 164
Diss. Lappeenranta University of Technology

ISBN 951-764-813-8, ISBN 951-764-819-7 (PDF)
ISSN 1456-4491

An accidental burst of a pressure vessel is an uncontrollable and explosion-like batch process. In this study it is called an explosion. The destructive effect of a pressure vessel explosion is relative to the amount of energy released in it. However, in the field of pressure vessel safety, a mutual understanding concerning the definition of explosion energy has not yet been achieved.

In this study the definition of isentropic exergy is presented. Isentropic exergy is the greatest possible destructive energy which can be obtained from a pressure vessel explosion when its state changes in an isentropic way from the initial to the final state. Finally, after the change process, the gas has similar pressure and flow velocity as the environment. Isentropic exergy differs from common exergy in that the process is assumed to be isentropic and the final gas temperature usually differs from the ambient temperature. The explosion process is so fast that there is no time for the significant heat exchange needed for the common exergy. Therefore an explosion is better characterized by isentropic exergy.

Isentropic exergy is a characteristic of a pressure vessel and it is simple to calculate. Isentropic exergy can be defined also for any thermodynamic system, such as the shock wave system developing around an exploding pressure vessel. At the beginning of the explosion process the shock wave system has the same isentropic exergy as the pressure vessel. When the system expands to the environment, its isentropic exergy decreases because of the increase of entropy in the shock wave. The shock wave system contains the pressure vessel gas and a growing amount of ambient gas.

The destructive effect of the shock wave on the ambient structures decreases when its distance from the starting point increases. This arises firstly from the fact that the shock wave system is distributed to a larger space. Secondly, the increase of entropy in the shock waves reduces the amount of isentropic exergy. Equations concerning the change of isentropic exergy in shock waves are derived.

By means of isentropic exergy and the known flow theories, equations illustrating the pressure of the shock wave as a function of distance are derived. A method is proposed as an application of the equations. The method is applicable for all shapes of pressure vessels in general use, such as spheres, cylinders and tubes. The results of this method are compared to measurements made by various researchers and to accident reports on pressure vessel explosions. The test measurements are found to be analogous with the proposed method and the findings in the accident reports are not controversial to it.

Keywords: Burst, energy, exergy, explosion, pressure vessel, shock wave
UDC 533.6.011.7 : 536.7 : 621.772 : 614.832

To Tiuku,
My Granddaughter

Acknowledgements

This study was carried out in the Energy Technology Department of Lappeenranta University of Technology, Finland, within the years of 1996 to 2003.
The idea for this study arose from my work as a safety engineer in the field of pressure vessel safety at Technical Inspection Centre, Finland (TTK), nowadays Safety Technology Authority, Finland (TUKES).
My supervisor, Professor Pertti Sarkomaa, who provided me with valuable guidance throughout the research, deserves my sincere thanks for encouraging me and believing in my ideas.
I would like to thank Mrs Riitta Viikari for helping me in finding information and Mrs Paula Välilä for editing the text. My special thanks go to my dear Marja for her patience and support during these years.

Heikki Kurttila
November, 2003
Helsinki, Finland

Contents **Page**

Symbols

Symbol	Description	Dimension
Latin alphabets		
a	sound velocity	m/s
B	exergy	J
C	constant factor	-
c	specific heat capacity	J/kgK
E	isentropic exergy	J
H	enthalpy	J
h	specific enthalpy	J/kg
k	compressibility	1/Pa
L	length	m
m	mass	kg
n	exponent	-
$\bar{P}$	relative overpressure by Baker	-
p	pressure	Pa
r	radius	m
$\bar{R}$	relative starting distance by Baker	-
S	entropy	J/K
s	specific entropy	J/kgK
T	temperature	K
t	time	s
Tr	transition point	-
U	internal energy	J
u	specific internal energy	J/kg
u	wave velocity	m/s
V	volume	m^3
W	work	J
w	flow velocity	m/s
x	distance	m
x	parameter	-

y	function	-

Greek alphabets

ε	loss ratio of isentropic exergy	-
κ	adiabatic factor	-
ρ	density	kg/m^3

Sub-indexes

a	ambience
ac	ambient gas captured into the shock wave system
L	pressurized part of the shock tube
M	mega-system
p	constant pressure
r	reflected wave
s	steady flow or system
T	table
t	change of time
u	unsteady flow
V	constant volume
x	transition point or difference between the ends of a gas element
0	equilibrium state with the ambience
1	beginning, starting point or state
2	end or state

Differentials and differences

D	differential of shock wave
d	differential
δ	partial differential
Δ	difference or change

1 Introduction

1.1 Background

There are many kinds of pressure vessels operating in the world, used for several purposes such as gas bottles, power plants, process industry, etc. An operating pressure vessel has contents with overpressure in proportion to the environment. That is why there are remarkable tensions concentrated on the wall structures of the vessel. The pressure vessels are designed and built so that they can carry the intended overpressure. Usually, pressure vessels contain a major force and a huge amount of energy. Practical experiences have shown that this fact cannot be detected by human senses.

The main risk concerning a pressure vessel is that, for some reason or other, the structure of the pressure vessel fails and the content discharges violently out of the vessel. The discharge is usually an explosion-like process causing destruction to the environment. There are many causes to make a pressure vessel explosion possible, such as exceeding the highest allowable pressure, corrosion, fatigue, etc. In order to avoid the hazards the pressure vessels are subject to close safety orders and inspections.

The definition of a risk of an accident is its probability multiplied by its impact. In this study the impacts are discussed. It is necessary to know the magnitude of the consequences of the pressure vessel explosion to be able to evaluate and manage the risks on the environment.

The accidental burst of a pressure vessel is an uncontrollable and explosion-like batch process. It is an unsteady process in which a huge amount of energy is released in a very short time (one second at the most). The characteristics of an explosion can be observed with the help of the theories of thermodynamics and compressible flow.

The explosion of a pressure vessel is somehow similar to that of an explosive. The main destructive effects of the explosion are shock waves, missiles and shaking. The explosion of a pressure vessel containing combustible liquid gas causes additionally fatal heat radiation and fire.

The factors of the shock wave affecting the magnitude of the destruction are overpressure and its impulse. An impulse is a time integral of the overpressure caused by an explosion. Also the negative pressure and its impulse are significant. According to reports, a building will break down only when both the pressure and the impulse of the shock wave exceed the

allowable levels [1]. If only one exceeds the level, the damages will not be significant. The pressure and the impulse decrease when the distance from the explosion point increases. The energy inside a pressure vessel is the essential factor in the effect of an explosion [2].

1.2 Objectives of the study

In this study the shock wave phenomena are discussed, but the missiles and the shaking are excluded. In the shock wave the overpressure is discussed but the impulse is excluded. The study concentrates on the pressure of the main shock wave as a function of the distance from the starting point in a hemispherically symmetric system. The problem is regarded to be three-dimensional or rather quasi-one-dimensional.

Many theories concerning the energy of pressure vessel explosion have been published in the field of pressure vessel safety [2]. In this work the theory of **"isentropic exergy "** will be found to be the best among the theories. Isentropic exergy is the greatest amount of mechanical energy which can be obtained from a system when its state changes isentropically into the state with the ambient pressure.

The idea of isentropic exergy seems to be poorly accepted in the field of pressure vessel safety [2]. However, although the idea of isentropic exergy seems to be generally known in the field of thermodynamics [3], the definition itself is new.

Isentropic exergy can be regarded as the property of a pressure vessel, and its amount is simple to calculate. However, isentropic exergy can also be applied to other thermodynamic systems, such as a shock wave system.

The aim of this study is to show the advantage of isentropic exergy in evaluating the pressure of a shock wave as a function of distance in a hemispherically symmetric system. The advantage of isentropic exergy is that with its help the pressure of a shock wave as a function of distance can be evaluated for pressure vessels of any shape in general use. Nowadays, even the most advanced theories evaluate the problem only for hemispherical pressure vessels, although, in general, they do not exist [2], [4].

The argument of this work is the following: During an accidental explosion, an expanding shock wave system develops outside the pressure vessel. The pressure vessel and the surrounding gas in the shock wave together produce a new expanding system. The system has obtained the initial isentropic exergy from the pressure vessel. However, the system loses

parts of its isentropic exergy all the time because of the increase of entropy in the shock waves. Finally, there is no isentropic exergy left, and the explosion is over. It is possible to picture an ideal explosion in which all the initial isentropic exergy will be lost in the shock waves and no destruction will occur. An example of this idea is illustrated in Figure 1.1.

In chapter 2 the basics of the explosion phenomena are discussed. The principal energy theories are presented and compared to each other. The isentropic exergy is chosen from the energy theories. The Rankine-Hugoniot equations and some of their consequences, such as the increases in post-shock temperature and entropy, are discussed. The one-dimensional shock tube theory is discussed, especially the state of the simple flow. It is essential to perceive the dual nature of the shock wave in a shock tube, the simple- and the non-simple states and the transition point between them. It is assumed in later chapters (3, 4 and 5) that the shock wave in the three dimensional case is of the same dual nature as in the shock tube. In chapter 2 the innovations are the calculated values of the isentropic exergy of pressure vessels and the derived equations concerning the loss of isentropic exergy in the shock waves.

In chapter 3 the equations concerning the pressure of the main shock wave as a function of the distance in a hemispherically symmetric system are derived. The equations are presented both for the simple and the non-simple states. For the simple state the equation is derived by applying the theories of thermodynamics, unsteady compressible flow and the Rankine-Hugoniot equations. The values of the shock wave pressure, the distance and the loss of isentropic exergy are presented in a table form. For the non-simple state the equation is derived by applying a simple self-similarity principle. This innovation accounts for the whole chapter 3.

In chapter 4 a method for the evaluation of the shock wave pressure as a function of distance in a hemispherically symmetric system is introduced. The method contains the equations derived in chapter 3. The transition point between the two above mentioned states is defined by comparing the results of the equations to the results of Baker's theory and the GRP-theory (GRP = Generalized Riemann Problem), which are the most advanced theories in the field [2], [4], [25]. These theories have been applied to spherical (in the air) or hemispherical (on the ground) pressure vessels. With the help of the method the function concerning the shock wave pressure as a function of the distance can be made also for a cylindrical pressure vessel.

In chapter 5 the proposed theory is compared with the test results of pressure vessel explosions carried out by three different researchers. The proposed theory is also compared with the findings in two different explosion accidents of pressure vessels.

The position of the transition point in a shock tube is discussed more closely in the appendix of this paper.

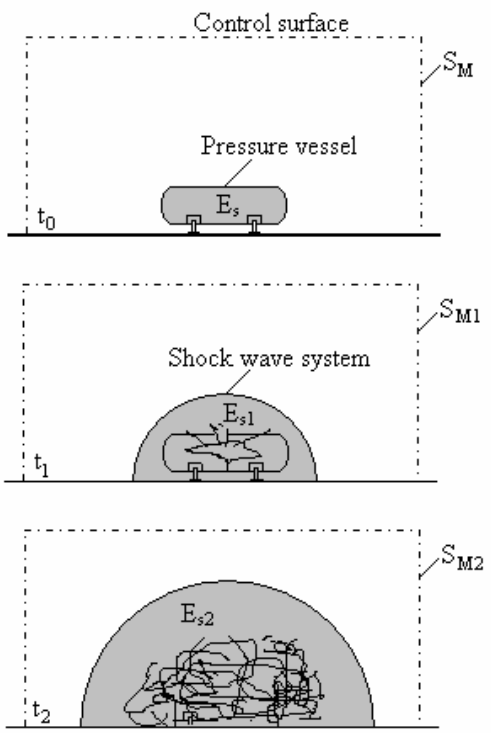

Fig. 1.1. Expansion of the shock wave caused by a pressure vessel explosion. The pressure vessel and a part of the ambient gas produce together a mega-system surrounded by a control surface. At the time t_0 the isentropic exergy in the pressure vessel is E_s and the entropy of the mega-system is S_M. At the time t_1 the developed shock wave system has the isentropic exergy E_{s1} and the entropy of the mega-system is S_{M1}. At the time t_2 the developed shock wave system has the isentropic exergy E_{s2} and the entropy of the mega-system is S_{M2}…
The entropy is increasing and the isentropic exergy is decreasing so that $S_M < S_{M1} < S_{M2}$ and $E_s > E_{s1} > E_{s2}$.

2 Explosion theories

2.1 Energy in pressure vessel explosion

Although the principal thermodynamic properties of pressure vessel explosion are generally known, there are differences in the theories of its energy. The main alternative theories are presented below.

2.1.1 Growth of internal energy caused by pressurization

The oldest theory is the growth of internal energy caused by pressurization in a constant volume. [2]. The pressurization is considered to happen by heating of the vessel gas from the outside or by combustion of the gas inside the pressure vessel. Brode has presented an equation on the change of the internal energy of a pressure vessel containing perfect gas [2]:

$$\Delta U = \frac{(p_1 - p_a)V_1}{\kappa - 1} \qquad (2.1.1)$$

where

ΔU = change of internal energy caused by the pressurization,

p_1 = pressure after the pressurization,

p_a = ambient pressure,

V_1 = volume of the pressure vessel,

κ = adiabatic constant of the gas.

This theory is very simple to apply. We only need to know the combustible energy of the gas or the heat energy from the outside. However, this theory does not express the effect of the explosion. Nevertheless, in very high values of pressure p_1 the energy result approximates with other theories. Baker has applied the theory for the calculation of the shock wave as a function of distance caused by a pressure vessel explosion [2]. The pressurization process and the increase of the internal energy are illustrated in a pV – diagram in Figure 2.1. As it can be seen in Figure 2.1, this theory does not express the effect of the explosion.

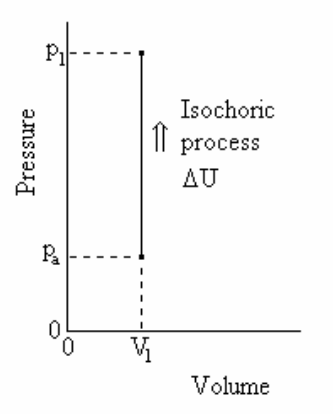

Fig. 2.1. Growth of internal energy by pressurization by heating the pressure vessel gas at constant volume. The arrow shows the direction of the process.

2.1.2 Work

When the gas with overpressure pushes a piston ahead it performs work. Equally, an explosion performs work outwards. The amount of work the expansive gas does can be presented as in the following equation:

$$W = \int_{V_1}^{V_2} pdV \qquad (2.1.2)$$

where

W = work,

p = pressure,

V_1 = volume in the beginning,

V_2 = volume in the end.

This theory is the most popular in the field of pressure vessel safety [5], [6], [7], [8], [9], [10], [11]. It is normal to imagine that the explosion energy is simply the work done by the isentropically expanding gas from a burst pressure vessel. However, all the work is not spent in the destruction caused by the explosion. Part of this work pushes the environmental atmosphere aside. All the work done by the expanding gas cannot be classified as explosion

energy, as then the theory would be in contradiction with the second law of thermodynamics. The work done by the pressure vessel gas is illustrated in Figure 2.2.

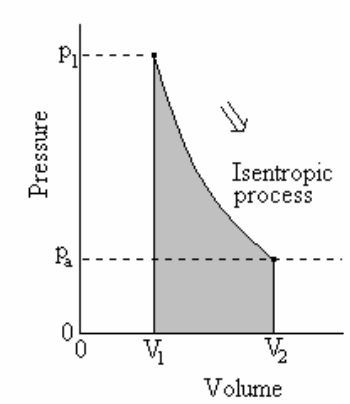

Fig. 2.2. Work done by the pressure vessel gas. The amount of work is coloured grey. The arrow shows the direction of the process.

2.1.3 Exergy

Exergy is the maximum amount of mechanical energy or an equivalent, such as electric energy, which can be obtained from a system while it changes from its initial state to the state in equilibrium with the environment. Exergy depends both on the state of the system and on the state of the environment. The equation for the exergy of a system in a batch process is:

$$B = U_1 - U_0 + p_a(V_1 - V_0) - T_a(S_1 - S_0) \qquad (2.1.3)$$

where

B = exergy,

U_1 = initial internal energy,

U_0 = internal energy in the equilibrium state with the environment,

V_1 = initial volume,

V_0 = volume in the equilibrium state with the environment,

S_1 = initial entropy,

S_0 = entropy in the equilibrium state with the environment,

p_a = ambient pressure,

T_a = ambient temperature.

In an exergic process the disequilibrium of the initial state of the system compared to the environment is changed to mechanical energy in the maximal way. Then the end values of the system gas become similar to those of the environment, as to the pressure and the temperature. The process where the exergy is achieved is illustrated in a pV –diagram in Figure 2.3.

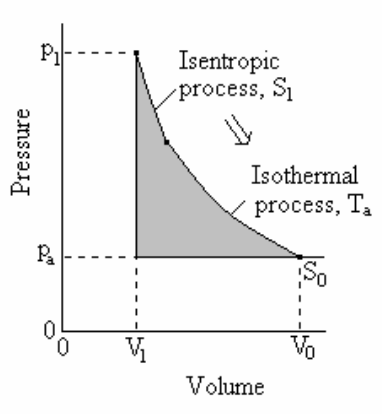

Fig. 2.3. Process where exergy is achieved. The amount of exergy is coloured grey. The arrow shows the direction of the process.

Crowl (1992) has suggested that exergy can be applied to explosions, as well [12]. However, exergy is an ideal theory of the maximum obtainable mechanical energy, and in order to approach it even close, extremely effective heat exchangers and sometimes advanced thermodynamic machines would be needed. An accidental explosion is an uncontrollable and fast process, however, and no significant heat exchange may occur. That is why the theory of exergy is not applicable in an explosion case. Here a theory describing a simpler process is needed.

2.1.4 Isentropic exergy

Isentropic exergy is the maximum amount of mechanical energy that can be obtained from a system while it changes isentropically from its original state to the state with the ambient pressure. This idea is commonly accepted in the field of thermodynamics [3]. In the field of

process safety this kind of idea has been presented by Baum and Fullard [13], [14], [15] and the present writer [16].

$$E = U_1 - U_2 - p_a(V_2 - V_1) \qquad (2.1.4)$$

where

E = isentropic exergy,

U_1 = internal energy in the beginning,

U_2 = internal energy in the end,

V_1 = volume in the beginning,

V_2 = volume in the end,

p_a = ambient pressure.

Because the process is considered isentropic and no heat exchange is assumed, equation (2.1.4) differs from equation (2.1.3). In equation (2.1.4) the part with the entropy values and the ambient temperature is eliminated because its value is null. Usually the final temperature of the gas differs from the ambient one. The final state of the gas is marked as U_2 and V_2. A process where the isentropic exergy is achieved is illustrated in a pV –diagram in Figure 2.4.

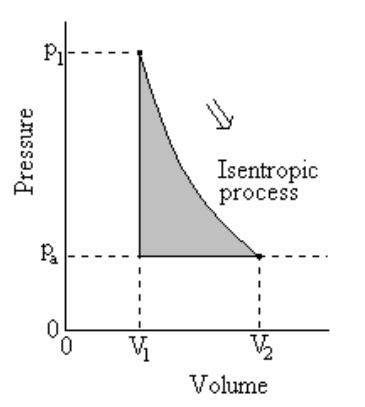

Fig. 2.4. Process where isentropic exergy is achieved. The amount of isentropic exergy is coloured grey. The arrow shows the direction of the process.

Equation (2.1.4) can be expressed also with the help of the enthalpies as follows:

$$E = H_1 - H_2 - V_1(p_1 - p_a) \qquad (2.1.5)$$

where

H_1 = enthalpy in the beginning,

H_2 = enthalpy in the end.

The practical form is in the specific values:

$$E = \frac{V_1}{v_1}(h_1 - h_2) - V_1(p_1 - p_a) \qquad (2.1.6)$$

where

h_1 = specific enthalpy in the beginning,

h_2 = specific enthalpy in the end.

v_1 = specific volume in the beginning.

In the case of ideal gas the equation can be expressed as:

$$E = \frac{\kappa}{\kappa - 1} p_1 V_1 \left[1 - \left(\frac{p_a}{p_1} \right)^{\frac{\kappa - 1}{\kappa}} \right] - V_1(p_1 - p_a) \qquad (2.1.7)$$

where

κ = adiabatic constant of the gas.

The equation of isentropic exergy (2.1.7) can also be expressed in an integral form as follows:

$$E = \int_1^2 (p - p_a) dV \qquad (2.1.8)$$

Isentropic exergy can also be applied into weakly compressible liquids, such as water:

$$E = ½ k V_1 (p_1 - p_a)^2 \qquad (2.1.9)$$

where

k = compressibility (for water k = 4.591×10^{-10} 1/Pa) [17].

The values of the isentropic exergy per volume in some pressure vessels as a function of overpressure are presented in Figure 2.5. The calculations of saturated liquids and steams have been carried out with the help equation (2.1.6) and Mollier-tables [18], [19]. For pressure vessels containing air the calculations have been done with equation (2.1.7) by using the adiabatic factor value $\kappa = 1.4$. For pressure vessels containing water with temperature below 100 ^{o}C the calculations have been done with equation (2.1.9) by using the compressibility $k = 4.591 \times 10^{-10}$ 1/Pa.

2.1.5 Comparison of the energy theories

In very high explosion pressures the amounts of energies become close to each other. However, in small overpressures the differences between the theories are significant. The theories are compared in Figure 2.6.

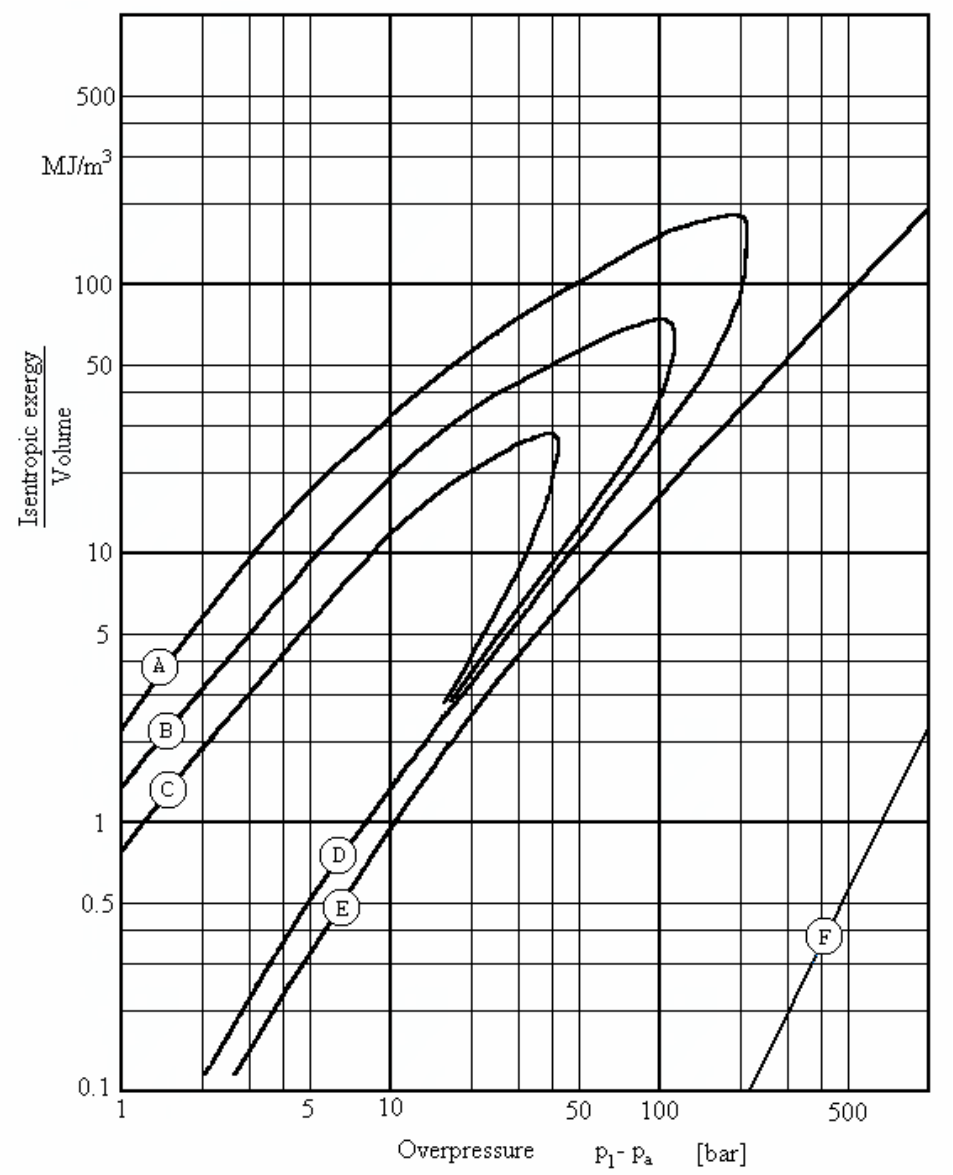

Fig. 2.5. Isentropic exergy per volume of a pressure vessel as a function of overpressure
A) Saturated liquid water from equation (2.1.6),
B) Saturated liquid ammonia from equation (2.1.6),
C) Saturated liquid propane from equation (2.1.6),
D) Saturated steams of water, ammonia and propane from equation (2.1.6),
E) Air from equation (2.1.7)
F) Water with temperature below 100 ^{o}C from equation (2.1.9).

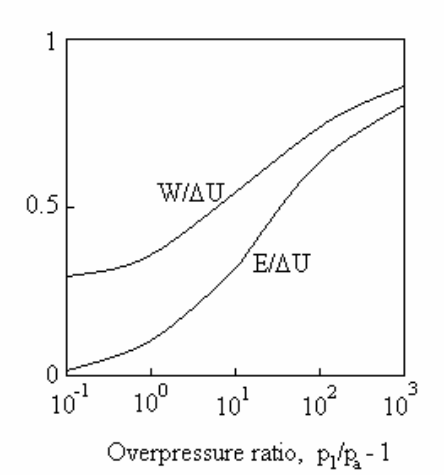

Fig. 2.6 Comparison of the results of different theories as functions of the overpressure ratio, p_1/p_a-1: Isentropic exergy is E, work is W and change of internal energy is ΔU.
Here the contents of the pressure vessels were chosen to be ideal gas with the adiabatic factor $\kappa = 1.4$.

2.2 Characteristics of the shock wave

2.2.1 Rankine-Hugoniot equations

Rankine and Hugoniot have independently derived equations for a shock wave in perfect gas [20], [21]. The equation for the density ratio in a shock wave is:

$$\frac{\rho_1}{\rho_a} = \frac{(\kappa+1)p_1 + (\kappa-1)p_a}{(\kappa-1)p_1 + (\kappa+1)p_a} \qquad (2.2.1)$$

where

ρ_1 = density in the shock wave,

ρ_a = ambient density,

p_1 = pressure in the shock wave,

p_a = ambient pressure,

κ = adiabatic factor.

The Rankine-Hugoniot equation for the velocity of the shock wave in a stagnant ambient gas u is:

$$u = \sqrt{\frac{(\kappa+1)p_1 + (\kappa-1)p_a}{2\rho_a}} \tag{2.2.2}$$

The corresponding Rankine-Hugoniot equation for the velocity of the gas in the shock wave w is:

$$w = \sqrt{\frac{2}{\rho_a[(\kappa+1)p_1 + (\kappa-1)p_a]}}(p_1 - p_a) \tag{2.2.3}$$

2.2.2 Post-shock temperature

When a shock wave reaches the part of ambient air the temperature ratio becomes the following:

$$\frac{T_1}{T_a} = \frac{p_1\rho_a}{p_a\rho_1} \tag{2.2.4}$$

where

T_1 = temperature in the shock wave,

T_a = ambient temperature.

By substituting the Rankine-Hugoniot equation (2.2.1) into (2.2.4) we get the temperature ratio in the shock wave:

$$\frac{T_1}{T_a} = \frac{(\kappa-1)p_1 + (\kappa+1)p_a}{(\kappa+1)p_1 + (\kappa-1)p_a} \cdot \frac{p_1}{p_a} \tag{2.2.5}$$

If there are no more shock waves the pressure of the air decreases eventually back to the ambient pressure in an isentropic way. Lord Rayleigh (1910) has indicated that the pressure of

the gas passing the shock front can only increase but never decrease [22]. The decrease of the pressure is essentially isentropic. Then the temperature ratio in the process of decreasing pressure becomes:

$$\frac{T_2}{T_1} = \left(\frac{p_a}{p_1} \right)^{\frac{\kappa-1}{\kappa}} \tag{2.2.6}$$

where

T_2 = post-shock temperature at the ambient pressure.

After substituting equation (2.2.5) by (2.2.6) and editing the post shock temperature equation (2.2.7) can be achieved:

$$\frac{T_2}{T_a} = \frac{(\kappa-1)p_1 + (\kappa+1)p_a}{(\kappa+1)p_1 + (\kappa-1)p_a} \cdot \left(\frac{p_1}{p_a} \right)^{\frac{1}{\kappa}} \tag{2.2.7}$$

Kinney has earlier presented an equation like (2.2.7) [5]. A shock wave process with an isentropic process into the post-shock state is illustrated in Ts -diagram in Figure 2.7.

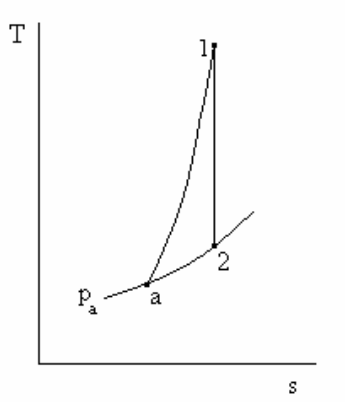

Fig. 2.7. States of ambient gas caused by a shock wave. a = ambient state, 1 = shock wave state, 2 = post-shock state, p_a = ambient pressure, T = temperature, s = specific entropy.

2.2.3 Change of entropy in a shock wave

Because the ambient temperature T_a and the post shock temperature T_2 take place at the same pressure p_a, the increase of the specific entropy $s_1 - s_a$ can be obtained from the basic equation of thermodynamics. For a finite process in a perfect gas the specific entropy changes as [21]:

$$s_1 - s_a = c_p \ln \frac{T_2}{T_a} \tag{2.2.8}$$

where

s_a = specific entropy of the ambient gas,

s_1 = specific entropy after the shock wave,

T_a = ambient temperature,

T_2 = post-shock temperature,

c_p = specific heat capacity at constant pressure.

By substituting equation (2.2.7) into (2.2.8), a formula for the specific entropy of perfect gas in a shock wave can be obtained:

$$s_1 - s_a = c_p \ln \left[\frac{(\kappa - 1)p_1 + (\kappa + 1)p_a}{(\kappa + 1)p_1 + (\kappa - 1)p_a} \left(\frac{p_1}{p_a} \right)^{\frac{1}{\kappa}} \right] \tag{2.2.9}$$

2.3 Change of isentropic exergy in a shock wave

2.3.1 Shock wave system

In this chapter equations concerning the change of isentropic exergy in shock waves are derived. Isentropic batch processes can roughly be divided into two classes: with shock waves and without them.

A batch process may be so slow that a shock wave is not developed. An example of this could be of a process where a cylinder with pressurized gas is pushing a piston ahead. The bar of the piston drives a dynamo, and electric energy is produced in it by the isentropic exergy of the cylinder gas. This arrangement is illustrated in Figure 2.8. In a process without a shock wave the isentropic exergy moves usually out from the system doing mechanical work into the environment. The process is schematically illustrated from the viewpoint of the system gas in Figure 2.9.

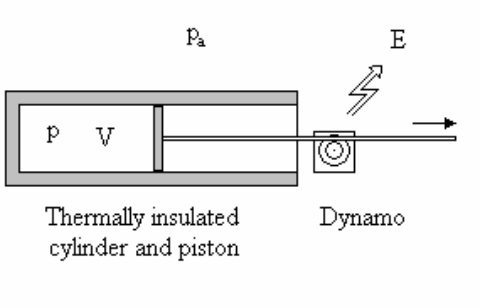

Fig. 2.8. Expansion process without a shock wave.
Isentropic exergy of a system producing electric energy.

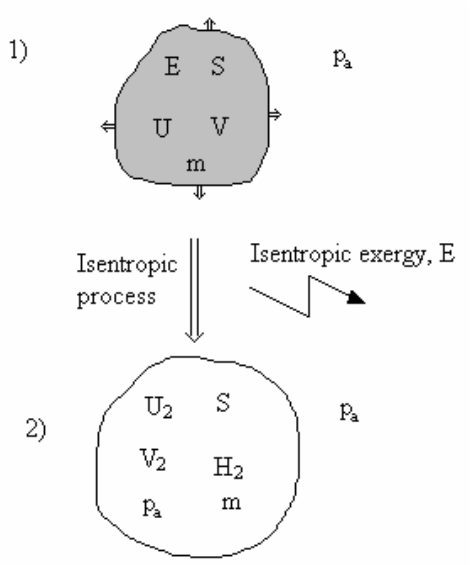

Fig. 2.9. Schematic diagram of a relatively slow isentropic expansion process. No shock wave exists. The interface of the system gas works as an expanding piston. The system including isentropic exergy is coloured grey. E = isentropic exergy, U = internal energy, V = volume, S = entropy, m = mass, p_a = ambient pressure, U_2 = final internal energy, V_2 = final volume, H_2 = final enthalpy.

On the other hand, an explosion process is usually so fast that it develops a shock wave around the system. The produced shock wave system can also give parts of its isentropic exergy to the environment causing mechanical work, such as destruction. However, in order to treat the shock wave problem theoretically, it is necessary to presume an ideal explosion process where no destructive work exists. The ideal shock wave system can be considered to keep its isentropic exergy to itself. The purpose is to study what will happen to isentropic exergy in this case.

In chapter 2.1.4 equation (2.1.4) concerning the isentropic exergy of a pressure vessel was obtained:

$$E = U_1 - U_2 + p_a(V_1 - V_2) \tag{2.1.4}$$

where

E = isentropic exergy of the pressure vessel,

U_1 = initial internal energy,

V_1 = initial volume,

U_2 = final internal energy,

V_2 = final volume,

p_a = ambient pressure.

Here U_1 and V_1 are substituted by temporary values of U and V. Here E means the actual value of the isentropic exergy.

Before the explosion process the pressure vessel gas is usually in a state of stagnation. After the process the gas reaches the final stagnation state, but between the stagnation states the system is in a dynamic state. It has also kinetic energy, when the internal energy U is regarded as the sum of the potential pressure energy and the kinetic energy. Usually, a shock wave system is not uniform. There exist distributions of specific internal energy u and flow velocity w. That is why the internal energy should be expressed with its specific values in an integral form:

$$U = \int_0^m \left(u + \frac{w^2}{2} \right) dm \tag{2.3.1}$$

where

m = mass of the system,

u = specific internal energy of a gas element,

w = velocity of a gas element.

In the final state the system gas has reached the ambient pressure p_a and there is no kinetic energy left. The final state of the system is usually not uniform. Usually, there are at least two types of gases: the system gas and the ambient gas. The final temperatures differ from each other, forming a distribution in the atmosphere. So, the final internal energy U_2 should be expressed in an integral form as:

$$U_2 = \int_0^m u_2 dm \tag{2.3.2}$$

where

u_2 = specific internal energy in the final state.

The shock wave system is assumed to keep the isentropic exergy to itself. However, the system is losing part of its isentropic exergy all the time because of the increase of entropy. Schematic diagrams of the process are given in Figure 1.1 in the introductory chapter and in Figure 2.10 in this chapter. A region of the ambient gas in the stagnant state around the system is presumed. The shock wave system and the ambient region together produce a mega-system surrounded by the control surface. No heat or mass transfer is presumed to cross the control surface. No heat transfer between the parts of the mega-system is presumed either. The volume of the mega-system is constant at the observed time.

The isentropic exergy E_M of the mega-system is similar to the shock wave system E and it can be expressed as:

$$E = (U + U_a) - (U_2 + U_a) + p_a[(V + V_a) - (V_2 + V_a)] \tag{2.3.4}$$

where

U_a = internal energy of the chosen ambient gas,

V_a = volume of the chosen ambient gas.

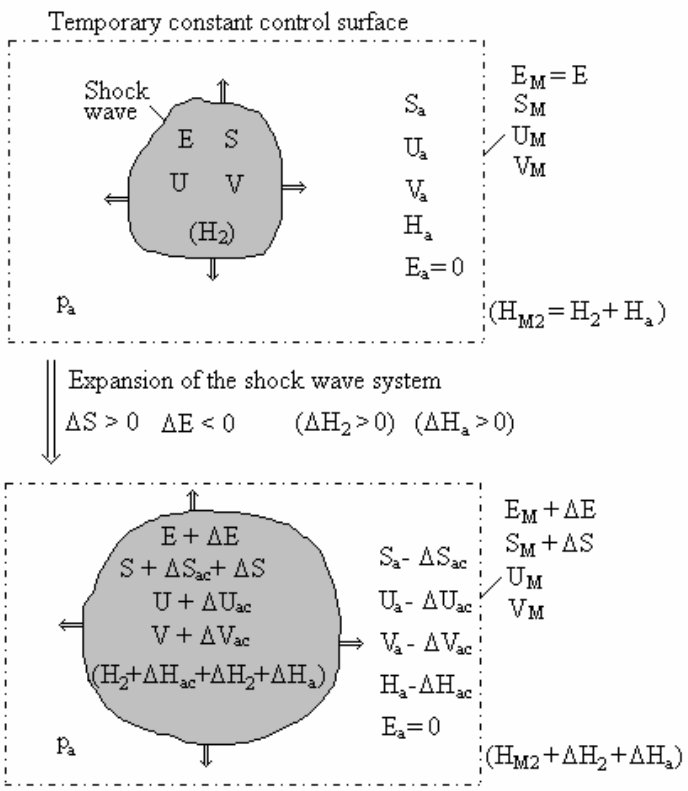

Fig. 2.10. Schematic diagram of an ideal shock wave system expanding into the environment. The expanding process takes place without any destructive work. The shock wave system is coloured grey. A region of the ambient volume is around the system surrounded by a control surface. The system and the ambient volume together produce a mega-system. The values of the shock wave system are isentropic exergy E, entropy S, internal energy U, volume V, post-shock enthalpy H_2. Corresponding values of the ambient gas are E_a (= 0), S_a, U_a, V_a, enthalpy H_a and pressure p_a. Corresponding values of the mega-system are: E_M (= E), S_M, U_M, V_M and H_{M2}. Values of the ambient gas captured into the shock wave system are ΔS_{ac}, ΔU_{ac}, ΔV_{ac} and ΔH_{ac} Changes in the process are isentropic exergy ΔE, entropy ΔS and post-shock enthalpies ΔH_2 and ΔH_a.

A change of the isentropic exergy ΔE can be presumed as the sum of all the changes as follows:

$$\Delta E = \Delta(U + U_a) - \Delta(U_2 + U_a) + p_a[\Delta(V + V_a) - \Delta(V_2 + V_a)] \qquad (2.3.5)$$

Because here the mega-system is assumed to be adiabatically insulated without a change of mass, mechanical energy or heat, we obtain:

$$\Delta(U + U_a) = 0 \tag{2.3.6}$$

During the observation time the mega-system volume stays constant:

$$\Delta(V + V_a) = 0 \tag{2.3.7}$$

By substituting equations (2.3.6) and (2.3.7) into (2.3.5) we obtain:

$$\Delta E = -\Delta(U_2 + U_a) - p_a \Delta(V_2 + V_a) \tag{2.3.8}$$

The basic definition of enthalpy, H, is:

$$H = U + pV \tag{2.3.9}$$

Thus equation (2.3.8) can be expressed through the changes of the post-shock enthalpy:

$$\Delta E = -\Delta H_2 - \Delta H_a \tag{2.3.10}$$

where

ΔH_2 = change of post-shock enthalpy in the initial shock wave system,

ΔH_a = change of post-shock enthalpy in the part of the ambient gas come into the shock wave system,

The isentropic exergy decreases as much as the post-shock enthalpy increases, as can be seen in equation (2.3.10). This fact is in harmony with the principle of the conservation law of energy.

After the shock process illustrated in Figure 2.10 the volume of the mega-system can be presumed to expand in an isentropic way, reaching the ambient pressure in all parts. In fact, the volume of the shock wave system only expands, because the pressures in it differ from the

ambient pressure. For the same reason the volume of the ambient part stays constant. All the changes in the gas values occur in the shock wave system only.

2.3.2 Effect of the main shock wave

The shock wave system is separated from the ambient gas by the main shock wave. Moreover, there exist other shock waves inside the system. This will be discussed further in chapter 2.3.4.

In this chapter the main shock wave on the outer surface is studied. Moreover, the greatest interest in this whole study is focuses on the main shock wave. It expands into the stagnant environment so that part of the ambient gas is captured by the shock wave system. Changes of isentropic exergy and post-shock enthalpy occur in the ambient gas simultaneously, when it comes into the shock wave system. The derivation is started by applying equation (2.3.10) as follows:

$$\Delta E = -\Delta H_a \tag{2.3.11}$$

In equation (2.3.11) the effects of other shock waves, ΔH_2, are neglected.

A differential small ambient gas element is assumed to be uniform. It is worth expressing the changes at a differential small form, as follows:

$$dE = -dH_a \tag{2.3.12}$$

In the case of ideal gas, equation (2.3.12) can be formulated into the form:

$$dE = -c_p(T - T_a)dm_a \tag{2.3.13}$$

where

c_p = specific heat capacity at constant pressure,

T = post-shock temperature,

T_a = ambient temperature,

dm_a = mass element of the ambient gas.

In basic thermodynamics the specific heat capacity in constant pressure c_p is defined as:

$$c_p = \frac{\kappa}{\kappa - 1}\frac{p}{\rho T} \tag{2.3.14}$$

where

p = pressure

ρ = density,

κ = adiabatic constant of the ambient gas.

By substituting equation (2.3.14) into (2.3.13) and by formulating it, equation (2.3.15) is obtained:

$$dE = -\frac{\kappa}{\kappa - 1} p_a \left(\frac{T}{T_a} - 1 \right) dV_a \tag{2.3.15}$$

In chapter 2.2 the post-shock temperature was presented in equation (2.2.7):

$$\frac{T_2}{T_a} = \frac{(\kappa - 1)p_1 + (\kappa + 1)p_a}{(\kappa + 1)p_1 + (\kappa - 1)p_a} \cdot \left(\frac{p_1}{p_a} \right)^{\frac{1}{\kappa}} \tag{2.2.7}$$

Here T_2 is the same as T in equation (2.3.15). By substituting equation (2.2.7) into (2.3.15) the change of the isentropic exergy caused by a shock wave can be obtained:

$$dE = -\frac{\kappa}{\kappa - 1} p_a \left[\frac{(\kappa - 1)p + (\kappa + 1)p_a}{(\kappa + 1)p + (\kappa - 1)p_a} \cdot \left(\frac{p}{p_a} \right)^{\frac{1}{\kappa}} - 1 \right] dV_a \tag{2.3.16}$$

The change of isentropic exergy depends effectively on the overpressure of the shock wave as presented in Figure 2.11.

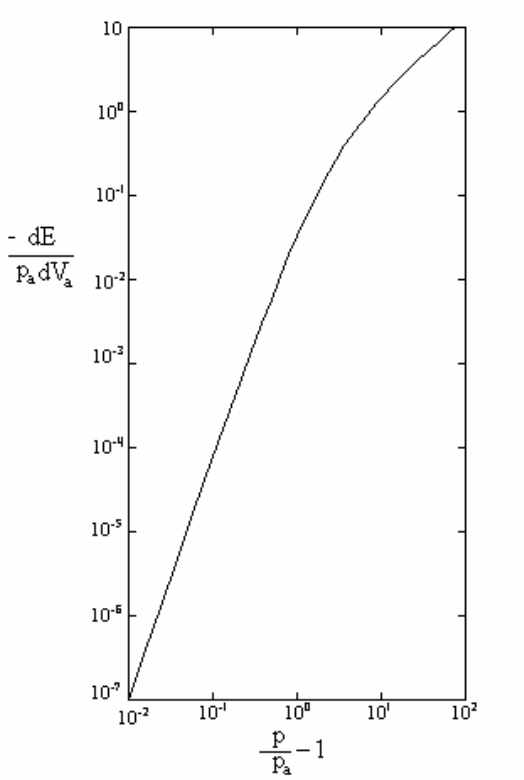

Fig. 2.11. Influence of the overpressure ratio of a shock wave to the change of isentropic exergy in two-atomic perfect gas. dE = change of isentropic exergy, p = pressure of the shock wave, p_a = ambient pressure, dV_a = volume expansion of the shock wave.

2.3.3 Cylinder and piston – one shock wave

In this chapter the change of isentropic exergy are verified again. A system is imagined to contain a cylinder and a piston moving with constant velocity in it. Perfect gas with a shock front is moving ahead the piston. At the same time there develops a vacuum state behind the piston. The cylinder-piston system is illustrated in Figure 2.12.

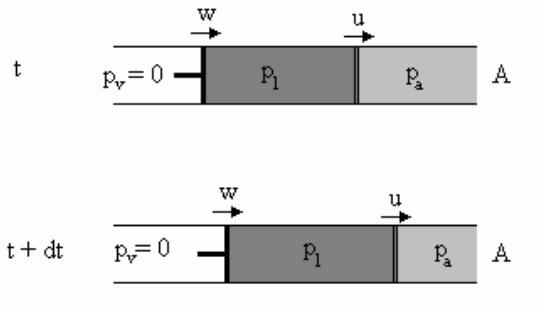

Fig. 2.12. Cylinder with a piston moving at constant velocity. p_a = ambient pressure, p_1 = shock wave pressure, p_v = pressure in the vacuum region (= 0), w = velocity of the piston and the gas, u = velocity of the shock wave, A = area of the cross section, t = time.

In the system the isentropic exergy includes isentropic pressure-exergy, work and kinetic energy. The balance of the changes in the isentropic exergy as a function of time difference dt can be expressed as follows:

$$-dE - dW + dE_{pv} + dE_p + dE_k = 0 \tag{2.3.17}$$

where

dE = change of the isentropic exergy,

dW = differential work done by the piston,

dE_{pv} = change of the isentropic exergy of the vacuum volume,

dE_p = change of the isentropic pressure-exergy of the shock wave gas,

dE_k = change of the kinetic energy of the shock wave gas.

If equation (2.3.17) is valid, then equation (2.3.16) concerning the change of isentropic exergy caused by a single shock wave is ratified. The application of equation (2.3.16) is the following:

$$dE = -\frac{\kappa}{\kappa - 1} p_a u \left[\frac{(\kappa - 1)p_1 + (\kappa + 1)p_a}{(\kappa + 1)p_1 + (\kappa - 1)p_a} \left(\frac{p_1}{p_a} \right)^{\frac{1}{\kappa}} - 1 \right] A dt \tag{2.3.18}$$

With the help of the Rankine-Hugoniot equations (2.2.1), (2.2.2) and (2.2.3), equation (2.3.18) can be formulated into a more practical form as follows:

$$dE = -\frac{\kappa}{\kappa-1} p_a u \left[\frac{u-w}{u} \left(\frac{p_1}{p_a} \right)^{\frac{1}{\kappa}} - 1 \right] A dt \tag{2.3.19}$$

The work done by the piston is:

$$dW = p_1 w A dt \tag{2.3.20}$$

The isentropic exergy of the pressure vessel including perfect gas was presented in equation (2.1.7):

$$E = \frac{\kappa}{\kappa-1} p_1 V_1 \left[1 - \left(\frac{p_a}{p_1} \right)^{\frac{\kappa-1}{\kappa}} \right] - V_1 (p_1 - p_a) \tag{2.1.7}$$

For the change of the isentropic pressure-exergy of the shock wave, equation (2.1.7) can be formulated into:

$$dE_p = p_a (u-w) \left[\frac{1}{\kappa-1} \frac{p_1}{p_a} - \frac{\kappa}{\kappa-1} \left(\frac{p_1}{p_a} \right)^{\frac{1}{\kappa}} + 1 \right] A dt \tag{2.3.21}$$

The isentropic pressure-exergy of the vacuum volume can be expressed with equation (2.3.21):

$$dE_{p_v} = p_a w A dt \tag{2.3.22}$$

The kinetic energy of the shock wave can be obtained as follows:

$$dE_k = \frac{\rho_1 w^2}{2} (u-w) A dt \tag{2.3.23}$$

where

ρ_1 = density of the gas in the shock wave.

With the help of equations (2.2.1), (2.2.2) and (2.2.3) equation (2.3.23) can be formulated into the form:

$$dE_k = \tfrac{1}{2}(p_1 - p_a)wAdt \tag{2.3.24}$$

By substituting equations (2.3.18), (2.3.19), (2.3.20), (2.3.21), (2.3.22), (2.3.23) and (2.3.24) into (2.3.17), the balance equation can be formed:

$$\frac{\kappa}{\kappa-1}p_a u\left[\frac{u-w}{u}\left(\frac{p_1}{p_a}\right)^{\frac{1}{\kappa}}-1\right]Adt - p_1 wAdt + p_a wAdt + p_a(u-w)\left[\frac{1}{\kappa-1}\frac{p_1}{p_a}-\frac{\kappa}{\kappa-1}\left(\frac{p_1}{p_a}\right)^{\frac{1}{\kappa}}+1\right]Adt$$
$$+\tfrac{1}{2}(p_1 - p_a)wAdt = 0 \tag{2.3.25}$$

By simplifying and formulating, equation (2.3.25) can be presented as:

$$p_1\left[-\frac{(\kappa+1)}{2}w+u\right]-p_a\left[\frac{(\kappa-1)}{2}w+u\right]=0 \tag{2.3.26}$$

According to the Rankine-Hugoniot equations (2.2.2) and (2.2.3) the following can be obtained:

$$\frac{w}{u}=\frac{2(p_1-p_a)}{(\kappa+1)p_1+(\kappa-1)p_a} \tag{2.3.27}$$

By substituting equation (2.3.27) into (2.3.26), the following is obtained:

$$p_1\left[-(\kappa+1)(p_1-p_a)+(\kappa+1)p_1+(\kappa-1)p_a\right]-p_a\left[(\kappa-1)(p_1-p_a)+(\kappa+1)p_1+(\kappa-1)p_a\right]=0 \tag{2.3.28}$$

By simplifying equation (2.3.28,) we obtain:

$$0 = 0 \tag{2.3.29}$$

Thus equation (2.3.16) is proved.

2.3.4 Effect of other shock waves

Usually, a shock wave system has also other shock waves besides the main one. Let us next observe a shock wave meeting the gas at a pressure differing from the ambient pressure. The process is illustrated in a T,s – diagram in Figure 2.13. To derive the equation concerning the change of isentropic exergy caused by an observed shock wave, equation (2.3.9) can be applied as follows:

$$dE_{12} = -c_p\left(T_{a2} - T_{a1}\right)dm \tag{2.3.30}$$

where

dE_{12} = change of isentropic exergy,

c_p = specific heat capacity at constant pressure,

T_{a1} = post-shock temperature at the ambient pressure without the observed shock wave,

T_{a2} = post-shock temperature at the ambient pressure after the observed shock wave,

dm = mass element.

Equation (2.3.30) can be formulated into the form:

$$dE_{12} = -\frac{\kappa}{\kappa - 1} p_a \left(\frac{T_{a2}}{T_{a1}} - 1 \right) dV_{a1} \tag{2.3.31}$$

where

p_a = ambient pressure,

dV_{a1}= post-shock volume element without the observed shock wave.

A gas system at a pressure differing from the ambient pressure is usually moving. So, the expansion velocity of the shock wave can be regarded as relative to the gas movement. Here the relative expansion volume of the shock wave dV_{11} in the gas at pressure p_1 is interesting. The volume element dV_{a1} at the ambient pressure is substituted by volume element dV_{11}. As the post-shock processes are essentially isentropic, we get:

$$dV_{a1} = dV_{11}\left(\frac{p_1}{p_a}\right)^{\frac{1}{\kappa}} \tag{2.3.32}$$

where

dV_{11} = volume element before the observed shock wave at pressure p_1,

p_1 = pressure where the observed shock wave meets the gas,

p_a = ambient pressure,

κ = adiabatic factor.

Because of the isentropic post-processes we get also:

$$\frac{T_{a2}}{T_{a1}} = \frac{T_{12}}{T_{11}} \tag{2.3.33}$$

where

T_{11} = temperature before the observed shock wave at pressure p_1,

T_{12} = post-shock temperature after the observed shock wave at pressure p_1.

Here equation (2.2.7) concerning the post-shock temperature can be applied as follows:

$$\frac{T_{12}}{T_{11}} = \frac{(\kappa-1)p_2 + (\kappa+1)p_1}{(\kappa+1)p_2 + (\kappa-1)p_1} \cdot \left(\frac{p_2}{p_1}\right)^{\frac{1}{\kappa}} \tag{2.3.34}$$

where

p_2 = pressure of the observed shock wave.

After substituting equations (2.3.32), (2.3.33) and (2.3.34) into (2.3.31), we get the intended equation.

$$dE_{12} = -\frac{\kappa}{\kappa-1} p_a \left(\frac{p_1}{p_a}\right)^{\frac{1}{\kappa}} \left[\frac{(\kappa-1)p_2 + (\kappa+1)p_1}{(\kappa+1)p_2 + (\kappa-1)p_1} \left(\frac{p_2}{p_1}\right)^{\frac{1}{\kappa}} - 1 \right] dV_{11} \qquad (2.3.35)$$

Equation (2.3.35) concerns the change of isentropic exergy caused by a shock wave meeting the gas at a pressure differing from the ambient pressure.

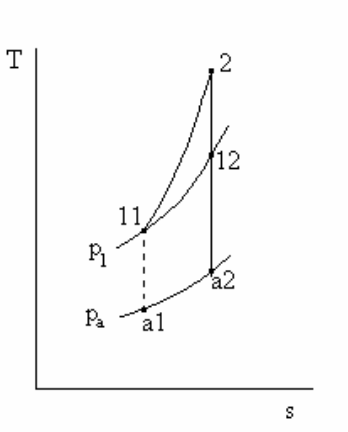

Fig. 2.13. A shock wave meeting the gas at the pressure differing from the ambient pressure. p_a = ambient pressure, p_1 = meeting pressure, 11 = meeting point, 2 = shock wave point, 12 = post-shock point at the meeting pressure, a2 = post-shock point at the ambient pressure, a1 = point after the virtual isentropic process at the ambient pressure without the shock wave in question.

2.4 Shock tube theory

2.4.1 Common theory

The theory of one-dimensional unsteady isentropic flow in a shock tube has been presented in several research papers [21]. The tube is divided into two parts by a wall between them: the first part has overpressure and the second part ambient pressure. Both parts contain perfect

gas in an equilibrium state. The overpressurized part of the tube represents the system. Suddenly the wall between the parts disappears and the gases begin to move due to the difference of the pressures. A shock wave starts at the point of the disappeared wall. The shock wave obeys the Rankine-Hugoniot equations, the velocity of the shock wave according to equation (2.2.2) and the gas flow velocity according to equation (2.2.3). The flow direction of the shock wave is towards the environmental part of the tube. At the same time a rarefaction wave develops in the system gas. The direction of the movement of the rarefaction wave movement is the opposite of the shock wave. The wave velocity of the top of the rarefaction wave is the same as the initial sound velocity -a_s.

2.4.2 Simple state

At first the rarefaction wave is in the simple state. This means that only one rarefaction wave exists there. The rarefaction wave has a distribution of sound velocity and flow velocity. The local flow velocity w depends on the local sound velocity a as follows:

$$w = \frac{2}{\kappa_s - 1}(a_s - a) \tag{2.4.1}$$

where

a_s = initial sound velocity,

κ_s = adiabatic factor of the gas.

The wave part having constant values of a and w has constant wave velocity u:

$$u = w - a \tag{2.4.2}$$

At the time t the wave part has reached position z:

$$z = ut = (w - a)t \tag{2.4.3}$$

The positions of the rarefaction waves in the simple state are schematically illustrated in Figure 2.14.

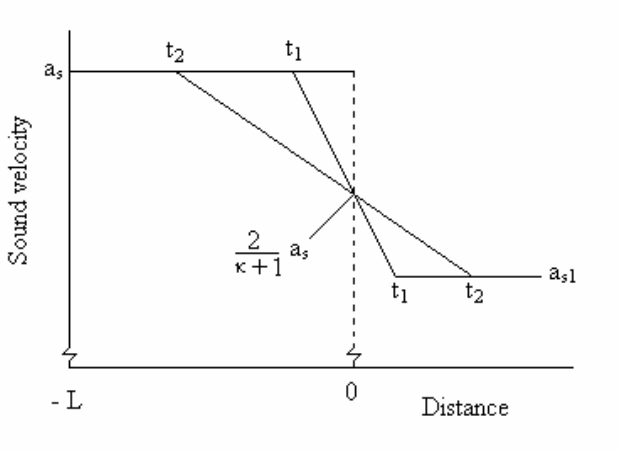

Fig. 2.14. Schematic diagram of the positions of a simple rarefaction wave at different times in a shock tube case. a_s = original sound velocity, a_{s1} = sound velocity equivalent with the shock wave pressure, t_1 and t_2 = times, κ = adiabatic constant, L = length of the pressurized part of the tube.

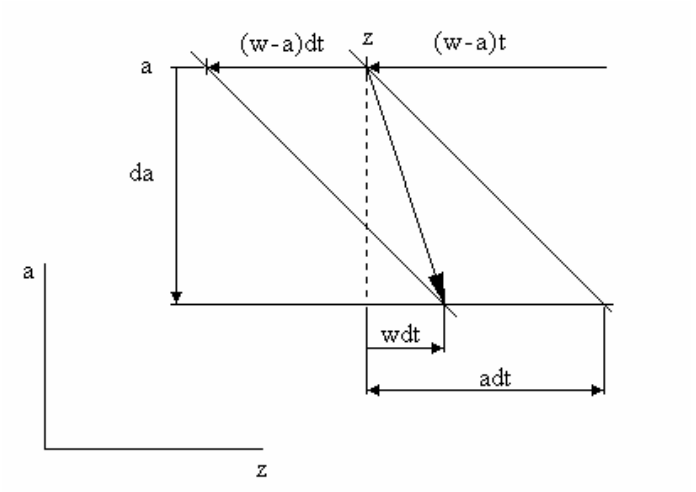

Fig. 2.15. Change of the sound velocity and the position of a gas element in the simple rarefaction wave in a shock tube. a = sound velocity, da = change of sound velocity, w = flow velocity, t = time, dt = change of time, z = position at the time t, z + wdt = position at the time t + dt.

When the length of a flowing gas element is chosen to be adt, then as shown in Figure 2.15 the change of the sound velocity at the time dt can be expressed as:

$$da = \delta_t a = \delta_x a \qquad (2.4.4)$$

where

$\delta_t a$ = change of the sound velocity in the gas element at time dt,

$\delta_x a$ = difference of the sound velocity between the ends of the element, adt.

Because the flow is isentropic, the equivalent changes of the pressure can be obtained as:

$$dp = \delta_t p = \delta_x p \tag{2.4.5}$$

Correspondingly, the equivalent changes of the flow velocity can be obtained as:

$$dw = \delta_t w = \delta_x w \tag{2.4.6}$$

2.4.3 Starting pressure of the shock wave

Immediately after the burst of a pressure vessel, a shock wave develops at the burst point. The shock wave consists of both the system gas and the ambient gas. At the starting point of the shock wave the pressure and the velocity of the gases are similar. The starting pressure of the shock wave is derived from the theories of shock tube, equation (2.4.1) and shock wave, equation (2.2.3). The derived equation is [1], [7]:

$$p_s = p_1 \left\{ 1 - \frac{a_a / a_s (\kappa_s - 1)(p_1 - p_a)}{\sqrt{2\kappa p_a [(\kappa + 1) p_1 + (\kappa - 1) p_a]}} \right\}^{\frac{-2\kappa_s}{\kappa_s - 1}} \tag{2.4.7}$$

where

p_s = initial pressure of the system,

p_1 = starting pressure of the shock wave,

p_a = ambient pressure,

a_s = sound velocity of the system gas in stagnation state,

a_a = ambient sound velocity,

κ_s = adiabatic factor of the system gas,

κ = adiabatic factor of the ambient gas.

The starting pressure of the shock wave, p_1, can be iterated from equation (2.4.7). Although the equation of the starting pressure has been derived with the help of the one-dimensional theory, it is valid in multi-dimensional cases, as well. The reason for this is that the flow dimensions in the starting point are small.

2.4.4 Dual nature of the shock wave

In the beginning of the shock tube process the propagated shock wave flows away from the cut point with the velocity u, as shown in equation (2.2.2). At the same time the rarefaction wave is induced into the opposite direction. Its top has the same velocity as the initial sound velocity but its value is negative, $-a_s$. The top of the induced rarefaction wave meets the end wall of the tube at time t_L, which can be obtained as:

$$t_L = \frac{L}{a_s} \tag{2.4.8}$$

where
L = length of the pressurized part of the tube.

After meeting the end wall the rarefaction wave is reflected back toward to the latter part of the induced wave. The reflected wave has accelerating velocity u_r:

$$u_r = w + a \tag{2.4.9}$$

where
w = local flow velocity in the induced wave,
a = local sound velocity in the induced wave.

The reflected wave velocity u_r accelerates to faster speed than the shock wave velocity u. Finally the reflected rarefaction wave reaches the shock wave. In this study the point where it occurs is called the transition point, x.

Before the meeting the shock wave has constant pressure and flow velocity, and it is in the simple state. When passing the transition point, the shock wave changes to a non-simple state where it has decreasing pressure and flow velocity. Gradually, the overpressure and the flow velocity become closer to null.

This is evident, because before the process the shock tube had a limited amount of isentropic exergy. However, it decreases in the shock wave according to equation (2.3.17). That is why the pressure of the shock wave cannot be constant forever. The behaviour of the gases in a shock tube is illustrated in Figure 2.16.

The position of the transition point in a shock tube is discussed in the appendix, where it is shown that in low overpressures of the shock waves (p/p_a-1 is below 0.2…0.5) the values of the loss ratio of the isentropic exergy in the simple state seem to be relatively constant. This finding suggests that the value of the loss ratio in the simple state may be constant in three-dimensional cases, as well.

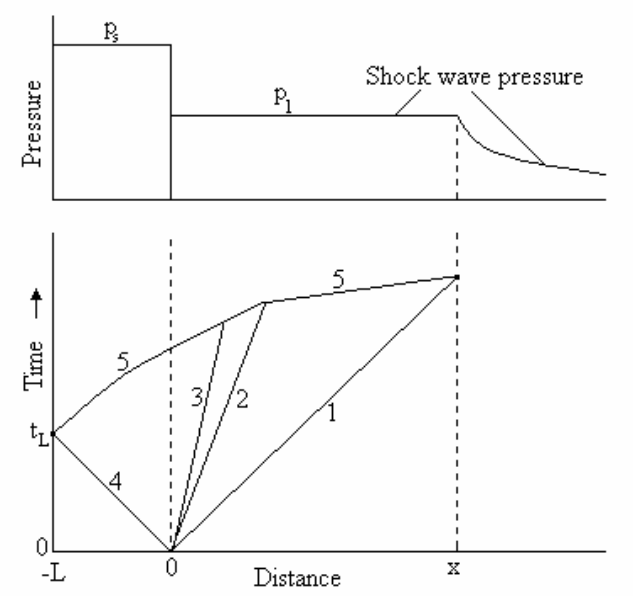

Fig. 2.16. Waves in a shock tube process. 1 = shock wave, 2 = interface of the system gas and the ambient gas, 3 = tail of the region where the pressure and the flow velocity are constant, 4 = top of the induced rarefaction wave, 5 = top of the reflected rarefaction wave, L = length of the pressurized part of the tube, x = transition point, t_L = time when the top of the induced rarefaction wave meets the back wall, p_s = initial pressure of the system, p_1 = pressure of the shock wave at the simple state.

3 Shock wave pressure as a function of distance in a hemispherically symmetric system

3.1 Simple state

In chapter 2 the one-dimensional shock tube theory was introduced. In the simple state the shock wave pressure was constant in the shock tube. In this chapter the shock wave pressure as a function of the distance in the simple state will be derived in space-angle-symmetric flow. The flow comes radially out from the origin as a quasi-one-dimensional flow.

In Figure 3.1 an element of perfect gas flowing away from the origin is illustrated in a radial duct with a space angle φ. The gas element is observed during the time difference dt. When the velocity of the element is w, its travel distance during the observing time dt is wdt. The acoustic velocity in the gas element is a. Here the thickness of the element has been chosen to be adt, which will prove to be useful later on.

At the observed moment t the values in the back side of the gas element are: radius r, pressure p, density ρ, sound velocity a, and flow velocity w. The corresponding values in the front side are: radius r + adt, pressure p + δ_xp, density ρ + δ_xρ, sound velocity a + δ_xa and flow velocity w +δ_xw.

At the observed moment t + dt, the values at the back of the gas element are: radius r + wdt, pressure p + δ_tp, density ρ + δ_t ρ, sound velocity a + δ_ta, and flow velocity w + δ_tw. The thickness of the gas element is (a + δ_xw)dt.

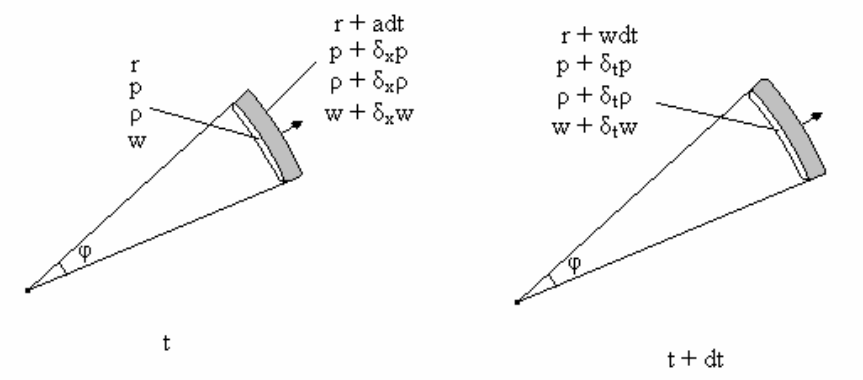

Fig. 3.1 Gas element in a radial flow

The flow is assumed to be isentropic. The derivation is made with the help of the conservation laws of mass and momentum.

3.1.1 Conservation law of mass

When moving in the duct the mass of the gas element stays constant:

$$\begin{aligned}&\varphi\left(\rho+½\delta_x\rho\right)\left(r+½adt\right)^2 adt\\&=\varphi\left(\rho+½\delta_x\rho+\delta_t\rho\right)\left(r+½adt+wdt\right)^2\left(a+\delta_x w\right)dt\end{aligned} \tag{3.1.1}$$

By simplifying, the equation can be presented in the form:

$$\frac{\delta_t\rho}{\rho}+\frac{\delta_x w}{a}+2\frac{wdt}{r}=0 \tag{3.1.2}$$

Because of the isentropic flow we obtain:

$$a^2=\frac{\delta_t p}{\delta_t\rho} \tag{3.1.3}$$

By substituting equation (3.1.3) into (3.1.2), it follows that:

$$\frac{\delta_t p}{\rho a^2}+\frac{\delta_x w}{a}+2\frac{wdt}{r}=0 \tag{3.1.4}$$

By formulating equation (3.1.4), we obtain:

$$\delta_t p+\rho a\delta_x w+2\rho a^2\frac{wdt}{r}=0 \tag{3.1.5}$$

3.1.2 Conservation law of momentum

With the help of Figure 3.1, the momentum equation can be constructed as:

$$\begin{aligned}&\varphi\left(p+\tfrac{1}{2}\delta_t p\right)(r+adt+\tfrac{1}{2}wdt)^2dt+\varphi\rho r^2awdt\\&=\varphi\left(p+\tfrac{1}{2}\delta_t p+\delta_x p\right)\left(r+adt+\tfrac{1}{2}wdt\right)^2dt+\varphi\rho r^2a\left(w+\delta_t w\right)dt\end{aligned} \tag{3.1.6}$$

By simplifying equation (3.1.6), it can be presented in the form:

$$\delta_x p+\rho a\delta_t w=0 \tag{3.1.7}$$

3.1.3 Dividing the flow into steady and unsteady components

The flow changes can be regarded as combinations of steady flow and unsteady flow:

$$\delta_t p=\delta_{ts}p+\delta_{tu}p \tag{3.1.8}$$

$$\delta_x p=\delta_{xs}p+\delta_{xu}p \tag{3.1.9}$$

$$\delta_t w=\delta_{ts}w+\delta_{tu}w \tag{3.1.10}$$

$$\delta_x w=\delta_{xs}w+\delta_{xu}w \tag{3.1.11}$$

Here sub-index s means steady flow and u means unsteady flow.

3.1.4 Steady flow

In a steady isentropic flow the changes in the gas are caused only by the change of the cross section in the duct. As the thickness of the gas element was chosen to be adt, the following equation is valid in the steady flow:

$$\frac{w}{a} = \frac{\delta_{ts} p}{\delta_{xs} p} = \frac{\delta_{ts} w}{\delta_{xs} w} \tag{3.1.12}$$

By substituting equation (3.1.12) into (3.1.5), the following form can be obtained:

$$\delta_{ts} p + \frac{\rho a^2}{w} \delta_{ts} w + 2\rho a^2 \frac{w dt}{r} = 0 \tag{3.1.13}$$

Also equation (3.1.7) can be presented in the following form:

$$\frac{a}{w} \delta_{ts} p + \rho a \delta_{ts} w = 0 \tag{3.1.14}$$

Equation (3.1.14) can be formulated as:

$$\frac{a^2}{w^2} \delta_{ts} p + \frac{\rho a^2}{w} \delta_{ts} w = 0 \tag{3.1.15}$$

By separating equation (3.1.15) from (3.1.13), we obtain:

$$\delta_{ts} p - \frac{a^2}{w^2} \delta_{ts} p + 2\rho a^2 \frac{w dt}{r} = 0 \tag{3.1.16}$$

By simplifying equation (3.1.16) we obtain:

$$\delta_{ts} p = -2\rho a^2 \frac{w^2}{w^2 - a^2} \frac{w dt}{r} \tag{3.1.17}$$

Equation (3.1.17) presents the pressure difference in a steady flow in the case where the observed length equals to the gas flow distance at time difference dt. In the case where the observed length equals to the chosen gas element, the pressure difference can be derived with the help of equations (3.1.5), (3.1.7) and (3.1.12) in the same way as equation (3.1.17):

$$\delta_{xs} p = -2\rho a^2 \frac{w^2}{w^2 - a^2} \frac{adt}{r} \tag{3.1.18}$$

As well as the equations (3.1.17) and (3.1.18), the equations concerning the gas velocity differences can be derived with the help of equations (3.1.5), (3.1.6) and (3.1.12). The following equations can be obtained:

$$\delta_{ts} w = 2 \frac{a^2 w}{w^2 - a^2} \frac{wdt}{r} \tag{3.1.19}$$

$$\delta_{xs} w = 2 \frac{a^2 w}{w^2 - a^2} \frac{adt}{r} \tag{3.1.20}$$

3.1.5 Unsteady flow

When a gas is in an imbalance state caused by pressure differences in its parts, it propagates an unsteady flow. Here the difference in the cross section of the flow has no influence on the unsteady flow component. It can be regarded as one-dimensional flow. In the shock tube theory, equations (2.4.5) and (2.4.6) concerning unsteady flow in a simple state were presented. Because the gas element was chosen to be adt, the following equations are in force in the simple state:

$$\delta_{xu} p = \delta_{tu} p \tag{3.1.21}$$

$$\delta_{xu} w = \delta_{tu} w \tag{3.1.22}$$

The sub-index u means that an unsteady flow is in question.

3.1.6 Pressure as a function of distance

By substituting equation (3.1.11) into (3.1.5), it can be presented in the form:

$$\delta_t p + \rho a\left(\delta_{xs} w + \delta_{xu} w\right) + 2\rho a^2 \frac{wdt}{r} = 0 \tag{3.1.23}$$

By substituting the flow components from equation (3.1.10) into (3.1.7), it can be obtained as:

$$\delta_x p + \rho a\left(\delta_{ts} w + \delta_{tu} w\right) = 0 \tag{3.1.24}$$

By decreasing equation (3.1.23) by (3.1.24) it follows that:

$$\delta_t p - \delta_x p + \rho a\left(\delta_{xs} w + \delta_{xu} w - \delta_{ts} w - \delta_{tu} w\right) + 2\rho a^2 \frac{wdt}{r} = 0 \tag{3.1.25}$$

Because of equation (3.1.22) we can simplify (3.1.25) into the form:

$$\delta_t p - \delta_x p + \rho a\left(\delta_{xs} w - \delta_{ts} w\right) + 2\rho a^2 \frac{wdt}{r} = 0 \tag{3.1.26}$$

By substituting equations of steady flow (3.1.19) and (3.1.20) into (3.1.26) it follows that:

$$\delta_t p - \delta_x p + 2\rho a \frac{a^2 w}{w^2 - a^2} \frac{adt}{r} - 2\rho a \frac{a^2 w}{w^2 - a^2} \frac{wdt}{r} + 2\rho a^2 \frac{wdt}{r} = 0 \tag{3.1.27}$$

By simplifying equation (3.1.27), we obtained:

$$\delta_t p - \delta_x p = -2\rho a^2 \frac{w}{a + w} \frac{wdt}{r} \tag{3.1.28}$$

By substituting the flow components from equation (3.1.8) into (3.1.5), it can be presented in the form:

$$\delta_{ts} p + \delta_{tu} p + \rho a \delta_x w + 2\rho a^2 \frac{wdt}{r} = 0 \tag{3.1.29}$$

By substituting the flow components from equation (3.1.9) into (3.1.7), it can be presented as:

$$\delta_{xs} p + \delta_{xu} p + \rho a \delta_t w = 0 \tag{3.1.30}$$

By decreasing equation (3.1.29) by (3.1.30) it follows that:

$$\delta_{ts} p + \delta_{tu} p - \delta_{xs} p - \delta_{xu} p - \rho a\left(\delta_t w - \delta_x w\right) + 2\rho a^2 \frac{wdt}{r} = 0 \tag{3.1.31}$$

By substituting equation (3.1.21) into (3.1.31), it can be simplified into the form:

$$\delta_{ts} p - \delta_{xs} p - \rho a\left(\delta_t w - \delta_x w\right) + 2\rho a^2 \frac{wdt}{r} = 0 \tag{3.1.32}$$

By substituting the equations of steady flow (3.1.17) and (3.1.18) into (3.1.32) it follows that:

$$-2\rho a^2 \frac{w^2}{w^2 - a^2} \frac{wdt}{r} + 2\rho a^2 \frac{w^2}{w^2 - a^2} \frac{adt}{r} - \rho a\left(\delta_t w - \delta_x w\right) + 2\rho a^2 \frac{wdt}{r} = 0 \tag{3.1.33}$$

By simplifying it, we obtain:

$$\delta_t w - \delta_x w = 2 \frac{a^2 w}{a + w} \frac{wdt}{r} \tag{3.1.34}$$

Equations (3.1.28) and (3.1.34) are connected with the shock wave equations. The pressure states of the gas element are presented in Figure 3.2. The element is touched by the shock

front. Dp is the pressure difference in the shock wave at the time dt. The following linear relationship between the pressure differences is explained in Figure 3.2:

$$Dp = \delta_t p + \frac{u-w}{a}\delta_x p \tag{3.1.35}$$

The corresponding difference of the gas velocity Dw is:

$$Dw = \delta_t w + \frac{u-w}{a}\delta_x w \tag{3.1.36}$$

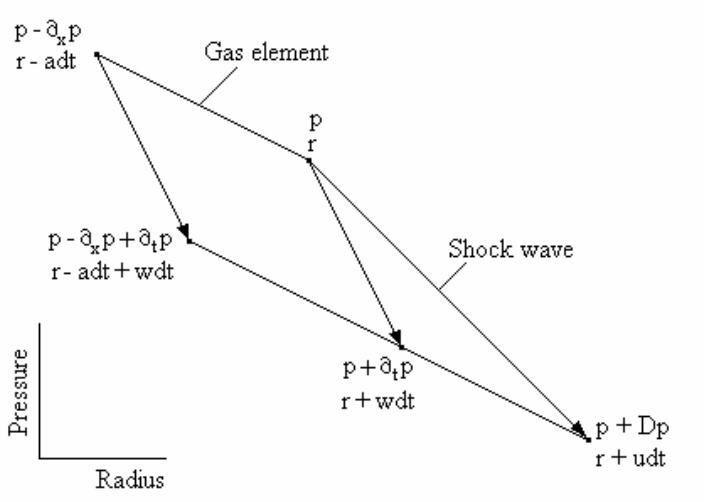

Fig. 3.2. Pressures in the gas element and the shock wave.

By substituting equations (3.1.35) and (3.1.36) into (3.1.5), it is obtained as:

$$Dp - \frac{u-w}{a}\delta_x p + \frac{\rho a^2}{u-w}Dw - \frac{\rho a^2}{u-w}\delta_t w + 2\rho a^2 \frac{wdt}{r} = 0 \tag{3.1.37}$$

By substituting equation (3.1.7) into (3.1.37), it can be presented as:

$$Dp+\rho a\frac{u-w}{a}\delta_t w+\frac{\rho a^2}{u-w}Dw-\frac{\rho a^2}{u-w}\delta_t w+2\rho a^2\frac{wdt}{r}=0 \tag{3.1.38}$$

By formulating it, we obtain:

$$Dp+\frac{\rho a^2}{u-w}Dw+\frac{(u-w)^2-a^2}{u-w}\rho\delta_t w+2\rho a^2\frac{wdt}{r}=0 \tag{3.1.39}$$

By substituting equation (3.1.35) into (3.1.28) it can be presented in the form:

$$Dp-\frac{u-w}{a}\delta_x p-\delta_x p=-2\rho a^2\frac{w}{a+w}\frac{wdt}{r} \tag{3.1.40}$$

By formulating we get:

$$Dp-\frac{a+u-w}{a}\delta_x p=-2\rho a^2\frac{w}{a+w}\frac{wdt}{r} \tag{3.1.41}$$

By substituting (3.1.7) we get:

$$Dp+\frac{a+u-w}{a}\rho a\delta_t w=-2\rho a^2\frac{w}{a+w}\frac{wdt}{r} \tag{3.1.42}$$

Equation (3.1.42) can be formulated as:

$$\delta_t w=-\frac{Dp}{\rho(a+u-w)}-\frac{2a^2w}{(a+w)(a+u-w)}\frac{wdt}{r} \tag{3.1.43}$$

By substituting equation (3.1.43) into (3.1.39), the term $\delta_t w$ can be eliminated:

$$Dp+\frac{\rho a^2}{u-w}Dw-\frac{(u-w)^2-a^2}{(u-w)\rho(a+u-w)}\rho Dp-\frac{2\rho a^2w}{(a+w)(a+u-w)}\frac{(u-w)^2-a^2}{u-w}\frac{wdt}{r}+2\rho a^2\frac{wdt}{r}=0$$

(3.1.44)

By simplifying equation (3.1.44), it can be presented in the form:

$$Dp + \rho a Dw + 2\rho a^2 \frac{w}{a+w}\frac{udt}{r} = 0 \tag{3.1.45}$$

The definition of udt can be expressed by the distance difference of the shock wave Dr as:

$$\frac{udt}{r} = \frac{Dr}{r} \tag{3.1.46}$$

The sound velocity in perfect gas is defined as:

$$\rho a^2 = \kappa p \tag{3.1.47}$$

By substituting equations (3.1.46) and (3.1.47) into (3.1.45), it can be put into the form:

$$Dp + \rho a Dw + 2\kappa p \frac{w}{w+a}\frac{Dr}{r} = 0 \tag{3.1.48}$$

In order to eliminate the difference of gas velocity Dw, it is necessary to use the Rankine-Hugoniot equation (2.2.3) of gas velocity in the shock wave:

$$w = \frac{2(p - p_a)}{\sqrt{2\rho_a[(\kappa+1)p + (\kappa-1)p_a]}} \tag{2.2.3}$$

The differential form of the gas velocity can be obtained by derivation as follows:

$$Dw = \frac{(\kappa+1)p + (3\kappa-1)p_a}{\sqrt{2\rho_a[(\kappa+1)p + (\kappa-1)p_a][(\kappa+1)p + (\kappa-1)p_a]}} Dp \tag{3.1.49}$$

The Rankine-Hugoniot equation (2.2.1) concerning the density in the shock wave is:

$$\rho = \rho_a \frac{(\kappa+1)p + (\kappa-1)p_a}{(\kappa-1)p + (\kappa+1)p_a} \tag{2.2.1}$$

By substituting equation (2.2.1) into (3.1.49), it can be written in the form:

$$Dw = \frac{(\kappa+1)p + (3\kappa-1)p_a}{\sqrt{2\rho[(\kappa-1)p + (\kappa+1)p_a][(\kappa+1)p + (\kappa-1)p_a]}} Dp \tag{3.1.50}$$

A part of equation (3.1.48) can be formulated into:

$$Dp + \rho a Dw = Dp + \rho\sqrt{\frac{\kappa p}{\rho}} \frac{(\kappa+1)p + (3\kappa-1)p_a}{\sqrt{2\rho[(\kappa-1)p + (\kappa+1)p_a][(\kappa+1)p + (\kappa-1)p_a]}} Dp \tag{3.1.51}$$

By simplifying it, we obtain:

$$Dp + \rho a Dw = \left\{1 + \frac{1}{2}\frac{(\kappa+1)p + (3\kappa-1)p_a}{(\kappa+1)p + (\kappa-1)p_a}\sqrt{\frac{2\kappa p}{(\kappa-1)p + (\kappa+1)p_a}}\right\} Dp \tag{3.1.52}$$

The rest of equation (3.1.48) can be given in the form:

$$2\kappa p \frac{w}{w+a}\frac{Dr}{r} = \kappa p \frac{4(p - p_a)}{2(p - p_a) + \sqrt{2\kappa p[(\kappa-1)p + (\kappa+1)p_a]}}\frac{Dr}{r} \tag{3.1.53}$$

By substituting equations (3.1.52) and (3.1.53) into (3.1.48), it can be presented as:

$$-\frac{Dr}{r} = \frac{1}{2}\left\{\frac{p - p_a}{\kappa p} + \sqrt{\frac{(\kappa-1)p + (\kappa+1)p_a}{2\kappa p}}\right\}\left\{1 + \frac{1}{2}\frac{(\kappa+1)p + (3\kappa-1)p_a}{(\kappa+1)p + (\kappa-1)p_a}\sqrt{\frac{2\kappa p}{(\kappa-1)p + (\kappa+1)p_a}}\right\}\frac{Dp}{p - p_a} \tag{3.1.54}$$

In the one-dimensional shock tube case the pressure of the shock wave is constant in the simple state. In the hemispherically symmetric case the pressure of the shock wave is variable according to equation (3.1.54).

3.1.7 Results

Usually, a shock wave moves in air where the value of the adiabatic factor κ is 1.4. In this case, equation (3.1.54) can be written in a simpler form:

$$-\frac{Dr}{r}=\frac{1}{2}\left(\frac{5}{7}\frac{p-p_a}{p}+\sqrt{\frac{p+6p_a}{7p}}\right)\left(1+\frac{3p+4p_a}{6p+p}\sqrt{\frac{7p}{p+6p_a}}\right)\frac{Dp}{p-p_a} \quad (3.1.55)$$

Equation (3.1.55) can be expressed in an integral form as:

$$-\int_{r_s}^{r}\frac{Dr}{r}=\frac{1}{2}\int_{p_1}^{p}\left(\frac{5}{7}\frac{p-p_a}{p}+\sqrt{\frac{p+6p_a}{7p}}\right)\left(1+\frac{3p+4p_a}{6p+p_a}\sqrt{\frac{7p}{p+6p_a}}\right)\frac{Dp}{p-p_a} \quad (3.1.56)$$

As the solution we get:

$$r=r_s\exp\left[\frac{1}{2}\int_{p}^{p_1}\left(\frac{5}{7}\frac{p-p_a}{p}+\sqrt{\frac{p+6p_a}{7p}}\right)\left(1+\frac{3p+4p_a}{6p+p_a}\sqrt{\frac{7p}{p+6p_a}}\right)\frac{Dp}{p-p_a}\right] \quad (3.1.57)$$

where

r = distance from the origin of the hemisphere,

r_s = radius of the pressure vessel,

p = pressure,

p_1 = starting pressure of the shock wave,

p_a = ambient pressure.

The solution of equation (3.1.57) has been calculated with the help of the Mathcad –program [29]. The results are presented in Figure 3.3 and in the table in Appendix 2.

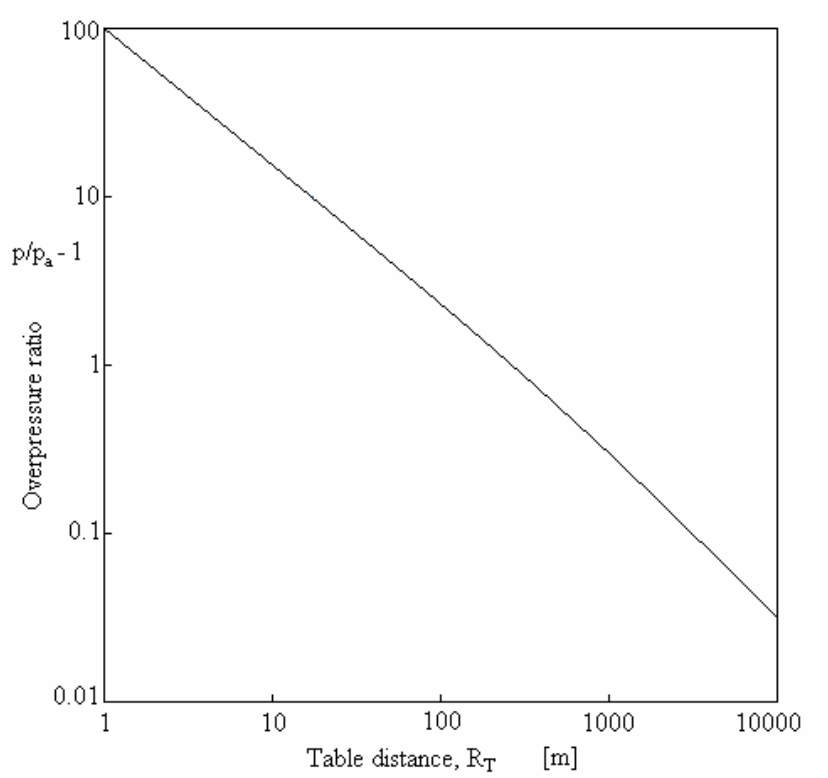

Fig. 3.3. Shock wave pressure as a function of distance in the simple state in air. p/p_a-1 is the overpressure ratio and R_T is the distance presented in the table in Appendix 2.

The table distance R_T and the cumulative loss of isentropic exergy E_T/p_a as a function of shock wave pressure p/p_a in air are presented in the table in Appendix 2, in which the explosion of a semi-spherical pressure vessel on the ground is assumed. The relative starting pressure of the explosion is chosen to be 101. The radius of the pressure vessel is chosen as 1 m. This is also the first value in the table in Appendix 2.

The cumulative loss ratio of the isentropic exergy per ambient pressure E_T/p_a should be calculated from equation (3.1.58), but in practice the values have been calculated by using the numerical integration method.

$$\frac{E_T}{p_a} = 7\pi \int_1^{R_T} \left[\frac{p/p_a + 6}{6p/p_a + 1} \left(\frac{p}{p_a} \right)^{\frac{1}{1.4}} - 1 \right] {R_T}^2 dR_T \qquad (3.1.58)$$

where

R_T = table value of the distance,

p/p_a = pressure ratio.

3.2 Non-simple state

3.2.1 System

In the case of the simple state discussed in chapter 3.1, isentropic exergy had no influence on the development of the shock wave pressure. However, in the case of the non-simple state the idea of isentropic exergy is extremely essential.

It was assumed in chapter 2.3.2 that all isentropic exergy will be lost in the main shock wave. During the explosion process, parts of the isentropic exergy take temporarily the form of kinetic energy. Then the isentropic exergy E contains potential pressure energy and kinetic energy.

The decrease of isentropic exergy is caused by the increase in the value in entropy in the shock waves. The loss process is assumed to occur in the main shock wave only. The part of the system flowing behind the main shock wave is assumed to move isentropically. During the process a gas element gives/gets isentropic exergy to/from the other elements in the system because of the changes in the pressures and the flow velocities. In the end, the shock wave system has expanded to the extreme and lost all the initial isentropic exergy. The loss of the isentropic exergy of a system caused by the main shock wave is illustrated in Figure 3.4.

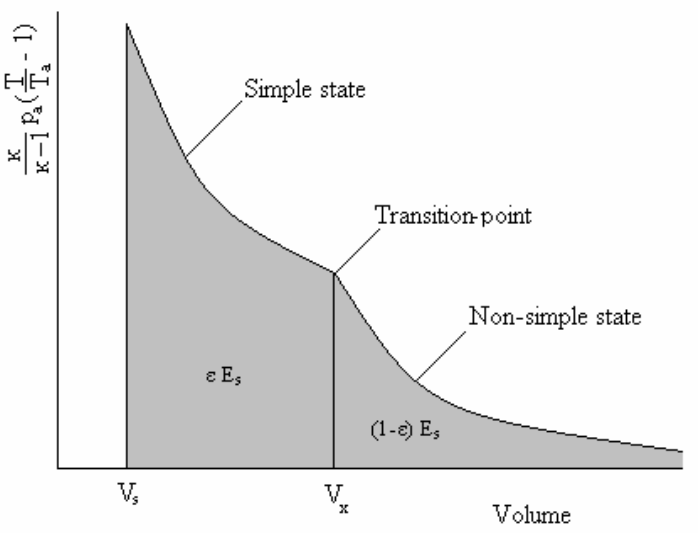

Fig. 3.4. Loss of the isentropic exergy of a system caused by the main shock wave. E_s = initial isentropic exergy of the pressure vessel, V_s = volume of the pressure vessel, V_x = transition volume, p_a = ambient pressure, T_a = ambient temperature, T = post-shock temperature, κ = adiabatic factor, ε = isentropic exergy ratio.

3.2.2 Change of isentropic exergy in a shock wave

A shock wave system produced as the result of a pressure vessel explosion gets the isentropic exergy from the vessel. The developing system loses its isentropic exergy gradually because of the progressive shock fronts, as equation (2.3.15) shows:

$$dE = -\frac{\kappa}{\kappa - 1} p_a \left(\frac{T}{T_a} - 1 \right) dV_a \qquad (2.3.15)$$

where

T = post-shock temperature,

T_a = ambient temperature

dV_a = volume change of the shock wave system.

In the non-simple state the isentropic exergy E decreases because of the expansion of the shock wave:

$$E = (1-\varepsilon)E_s - \frac{\kappa}{\kappa-1} p_a \int_{V_x}^{V} \left(\frac{T}{T_a} - 1 \right) dV_a \tag{3.2.1}$$

Equation (3.2.1) can be expressed with the volume ratio as:

$$E = (1-\varepsilon)E_s - \frac{\kappa}{\kappa-1} p_a V_x \int_{1}^{V/V_x} \left(\frac{T}{T_a} - 1 \right) d\left(\frac{V}{V_x} \right) \tag{3.2.2}$$

When the shock wave system expands into infinity, the isentropic exergy of the system closes in null:

$$E(\infty) = (1-\varepsilon)E_s - \frac{\kappa}{\kappa-1} p_a V_x \int_{1}^{\infty} \left(\frac{T}{T_a} - 1 \right) d\left(\frac{V}{V_x} \right) = 0 \tag{3.2.3}$$

3.2.3 Self similarity

When a process is too complicated to be studied analytically, a simple estimation theory, such as the self-similarity theory may be worth turning to. Many natural subjects obey the self-similarity principle, which means that in many cases the proportions between the parts of a system stay similar even if its dimensions change. When a system is losing its power (here isentropic exergy), its values usually approach null asymptotically. The type of the process must be known. A simple equation of self-similarity is the following [24]:

$$y = Cx^n \tag{3.2.4}$$

where

y = function,

x = parameter,

C = constant factor,

n = constant exponent.

In equation (3.2.4) function y is closing in null asymptotically while parameter x grows into infinity if the value of the exponent n is negative.

3.2.4 Application of self-similarity in shock waves

An application equation can be produced according the self similarity equation (3.2.4) as:

$$\frac{T}{T_a}-1=\left(\frac{T_x}{T_a}-1\right)\left(\frac{V}{V_x}\right)^n \tag{3.2.5}$$

where

T = post-shock temperature,

T_x = post-shock temperature in the transition point,

n = exponent.

By substituting equation (3.2.5) into (3.2.3), it can be written as:

$$(1-\varepsilon)E_s-\frac{\kappa}{\kappa-1}p_aV_x\left(\frac{T_x}{T_a}-1\right)\int_1^\infty\left(\frac{V}{V_x}\right)^n d\left(\frac{V}{V_x}\right)=0 \tag{3.2.6}$$

In the extremely large volume V the term $(V/V_x)^n$ approaches null. This fact is caused by the negative value of exponent n. The value below null of exponent n can be seen in Figure 3.4. Thus the solution of the integral equation (3.2.6) is:

$$(1-\varepsilon)E_s-\frac{\kappa}{\kappa-1}p_aV_x\left(\frac{T_x}{T_a}-1\right)\frac{0-1}{n+1}=0 \tag{3.2.7}$$

Exponent n can be obtained by formulating equation (3.2.7) as:

$$n=-\frac{\kappa}{\kappa-1}\frac{p_aV_x}{(1-\varepsilon)E_s}\left(\frac{T_x}{T_a}-1\right)-1 \tag{3.2.8}$$

In a (hemi-) spherically symmetric system equation (3.2.5) can be expressed with radius r and r_x:

$$\frac{T}{T_a}-1=\left(\frac{T_x}{T_a}-1\right)\left(\frac{r}{r_x}\right)^{3n} \tag{3.2.9}$$

The post shock temperature can be obtained from equation (2.2.7) as:

$$\frac{T_1}{T_a}=\frac{(\kappa-1)p_1+(\kappa+1)p_a}{(\kappa+1)p+(\kappa-1)p_a}\cdot\left(\frac{p_1}{p_a}\right)^{\frac{1}{\kappa}} \tag{2.2.7}$$

By substituting equation (2.2.7) into (3.2.9), it can be presented as:

$$\frac{(\kappa-1)p+(\kappa+1)p_a}{(\kappa+1)p+(\kappa-1)p_a}\left(\frac{p}{p_a}\right)^{\frac{1}{\kappa}}-1=\left[\frac{(\kappa-1)p_x+(\kappa+1)p_a}{(\kappa+1)p_x+(\kappa-1)p_a}\left(\frac{p_x}{p_a}\right)^{\frac{1}{\kappa}}-1\right]\left(\frac{r}{r_x}\right)^{3n} \tag{3.2.10}$$

In a hemispherically symmetric system the transition volume V_x is:

$$V_x=\frac{2\pi}{3}r_x{}^3 \tag{3.2.11}$$

Then exponent n can be obtained as:

$$n=-\frac{\kappa}{\kappa-1}\frac{2\pi r_x{}^3}{3}\frac{p_a}{(1-\varepsilon)E_s}\left[\frac{(\kappa-1)p_x+(\kappa+1)p_a}{(\kappa+1)p_x+(\kappa-1)p_a}\left(\frac{p_x}{p_a}\right)^{\frac{1}{\kappa}}-1\right]-1 \tag{3.2.12}$$

This theory will be applied in chapters 4 and 5.

4 Proposed method for defining the pressure of the shock wave as a function of the distance

4.1 Method

4.1.1 Basics

In this chapter the method for calculating the pressure of a shock wave as a function of the distance is developed. The method is proposed because all the details cannot be proved and uncertain assumptions have to be made, such as: a hemispherically symmetric shock wave, fast and large opening of the defect, neglecting the density of the opening pressure vessel wall, and inadequately proved value of ε. In fact, the proposed method just shows a possibility of how to apply the idea of isentropic exergy for evaluating the pressure of the shock wave as a function of the distance.

The pressure vessel is assumed to be situated on the ground and its shape can be anything in practical use, e.g. a sphere, cylinder or tube. The explosion is assumed to begin simultaneously and in a hemispherically symmetric way around a point in the cylinder axis of the pressure vessel. In the case of a cylinder or tube the explosion can be assumed to start at the most risky part of the cylinder.

The following data from the pressure vessel is needed for completely specifying the behaviour of the shock wave pressure as a function of the distance: the isentropic exergy of the pressure vessel E_s, the inner radius of the cylinder (or the sphere) r_s and the starting pressure of the shock wave p_1.

The shape of the pressure vessel is simulated by a hemispherical pressure vessel. It has the same inner radius as the cylinder or the sphere of the real pressure vessel. The initial values of the gas are similar in the virtual pressure vessel and the real one. The amount of the isentropic exergy in the virtual pressure vessel is presumed to be the same as in the real pressure vessel.

In the explosion process the shock wave is assumed to occur in two steps. The first step is the simple state and the second step is the non-simple state. Three particular points exist in the shock wave. In fact, they are hemispherical surfaces but are called points here. The initial point has the inner radius of the pressure vessel and the burst pressure p_s. The starting point has the same radius as the initial point, but its pressure is lower, starting pressure p_1. The

transition point separates the simple and non-simple states from each other. Actually, the transition point is virtual and in reality a smoother transition region may exist instead of it. The states and the points are depicted in Figure 4.1.

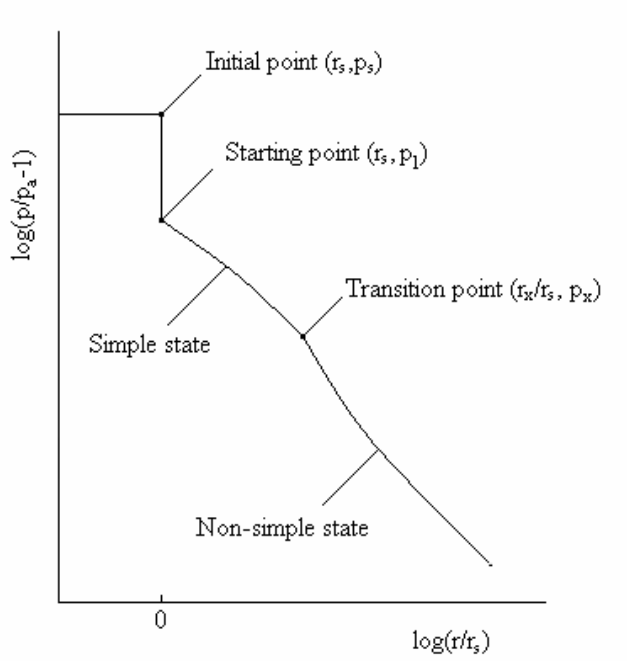

Fig. 4.1. Schematic diagram of the states and the points of the main shock wave caused by the explosion of a pressure vessel. The shape of the shock wave is hemispherical. p = pressure, p_a = ambient pressure, p_s = initial pressure, p_1 = starting pressure, p_x = transition pressure, r = distance, r_s = inner radius of the pressure vessel cylinder (or of the sphere if in question), r_x = transition distance.

4.1.2 Starting point

At first the starting pressure ratio of the explosion must be obtained. The starting pressure p_1 was presented in chapter 2.4.3 in equation (2.4.7):

$$p_s = p_1 \left\{ 1 - \frac{a_a / a_s (\kappa_s - 1)(p_1 - p_a)}{\sqrt{2\kappa p_a [(\kappa + 1)p_1 + (\kappa - 1)p_a]}} \right\}^{\frac{-2\kappa_s}{\kappa_s - 1}} \qquad (2.4.7)$$

where

p_s = initial pressure in the pressure vessel,

p_1 = starting pressure of the shock wave,

a_s = initial sound velocity of the pressure vessel gas,

a_a = sound velocity of ambient gas,

κ_s = adiabatic factor of the pressure vessel gas,

κ = adiabatic factor of ambient gas.

4.1.3 Simple state

The shock wave pressure as a function of distance in the simple state was derived in chapter 3.1, where equation (3.1.58) and Appendix table 2 were obtained. It is simpler to obtain the shock wave pressures and the distances by using the table in Appendix 2. With the help of the calculated starting pressure ratio p_1/p_a, the corresponding starting distance R_{T1} can be interpolated from the table. The real distance r can be obtained by the following equation:

$$r = r_s \frac{R_T}{R_{T1}} \tag{4.1.1}$$

where

R_T = table distance with pressure ratio p/p_a,

R_{T1} = table distance at the starting point,

r_s = inner radius of the pressure vessel cylinder (or sphere).

4.1.4 Transition point

In order to define the transition point, the cumulative loss of the isentropic exergy in the simple state $-\Delta E_x$ must be defined. The loss ratio of the isentropic exergy in the simple state can be marked by ε, which can be obtained from:

$$\varepsilon = \frac{-\Delta E_x}{E_s} \tag{4.1.2}$$

The value of ε will be discussed in chapter 4.2. The values of the transition point can be calculated with the help of the table in Appendix 2. Because of geometry, the table value of the cumulative loss of the isentropic exergy at the simple state E_{Tx} can be obtained from equation:

$$E_{Tx}/p_a = \left(\frac{R_{T1}}{r_s}\right)^3 \varepsilon E_s/p_a + E_{T1}/p_a \tag{4.1.3}$$

where

E_{T1} = table value of the cumulative loss of isentropic exergy at the starting distance.

The values on the transition point as p_x/p_a and R_{Tx} can be interpolated with E_{Tx} from the table in Appendix 2. The real transition distance can be obtained from equation:

$$r_x = \frac{R_{Tx}}{R_{T1}} r_s \tag{4.1.4}$$

4.1.5 Non-simple state

The equations for the non-simple state were discussed in chapter 3.2.4, where equations (3.2.10) and (3.2.12) were derived. The equation concerning the pressure of the shock wave as a function of the distance in the non-simple state was obtained as:

$$\frac{(\kappa-1)p+(\kappa+1)p_a}{(\kappa+1)p+(\kappa-1)p_a}\left(\frac{p}{p_a}\right)^{\frac{1}{\kappa}} - 1 = \left[\frac{(\kappa-1)p_x+(\kappa+1)p_a}{(\kappa+1)p_x+(\kappa-1)p_a}\left(\frac{p_x}{p_a}\right)^{\frac{1}{\kappa}} - 1\right]\left(\frac{r}{r_x}\right)^{3n} \tag{3.2.10}$$

The corresponding exponent n was obtained as:

$$n = -\frac{\kappa}{\kappa-1}\frac{2\pi r_x^{\,3}}{3}\frac{p_a}{(1-\varepsilon)E_s}\left[\frac{(\kappa-1)p_x+(\kappa+1)p_a}{(\kappa+1)p_x+(\kappa-1)p_a}\left(\frac{p_x}{p_a}\right)^{\frac{1}{\kappa}}-1\right]-1 \qquad (3.2.12)$$

4.2 ε – value and comparison with other theories

The loss ratio of the isentropic exergy in the simple state ε is considered to have a constant value in all cases. The idea of the constant value of ε is discussed in Appendix 1. In this chapter the idea of the constant value of ε is applied to three-dimensional shock waves, as well. It is sufficient to present the ε -value with one decimal, in this case.

The value of ε is chosen so that the theory presented here will be in harmony with other related theories. Comparisons are done for hemispherically symmetric pressure vessels on the ground and a spherically symmetric pressure vessel in the air.

After choosing the ε –value, a crude assumption will be made that the value of ε for defining the transition point is applicable to cylindrical pressure vessels, as well. This assumption will be tested by comparisons with the results of some real explosion tests.

4.2.1 Comparison with Baker's theory

Baker's theory was developed for hemispherical pressure vessels situated on the ground and containing perfect gas [2]. The theory is mentioned to be the most advanced theory in the field. It is reasonable for the ε -value to be based on Baker's theory, particularly when the shape of the pressure vessel is hemispherical.

Baker's theory is based on the diagram illustrated in Figure 4.3. There the relative starting distance $\overline{R}$ is defined with the explosion energy ΔU_V as:

$$\overline{R}_1 = r_s\left(\frac{p_a}{\Delta U_V}\right)^{\frac{1}{3}} \qquad (4.1.5)$$

where

r_s = radius of the hemispherical pressure vessel,

p_a = ambient pressure,

ΔU_V = increase of internal energy caused by pressurization as equation (2.1.1) shows.

At first the starting pressure of the shock wave must be defined from equation (2.4.7), just as in the proposed method. Baker has marked the ratio of the starting over-pressure with $\overline{P}_1$. With the help of $\overline{P}_1$ and $\overline{R}_1$ the line can be chosen from Figure 4.2.

Here the proposed theory is compared with Baker's theory and an adequate value of ε is chosen. Four examples of hemispherical pressure vessels have been calculated. The pressure vessels have the radius of 1 m and contain air. The initial over pressure ratios $p_s/p_a - 1$ have been chosen to be 10 and 100. The initial sound velocity ratios a_s/a_a have bee chosen to be 1 and 2. The values have been calculated as presented in chapter 4.1. The results of the proposed theory with ε-values of 0.05, 0.07 and 0.10 have been compared with the corresponding results of Baker. The results are presented in Figures 4.3, 4.4, 4.5 and 4.6.

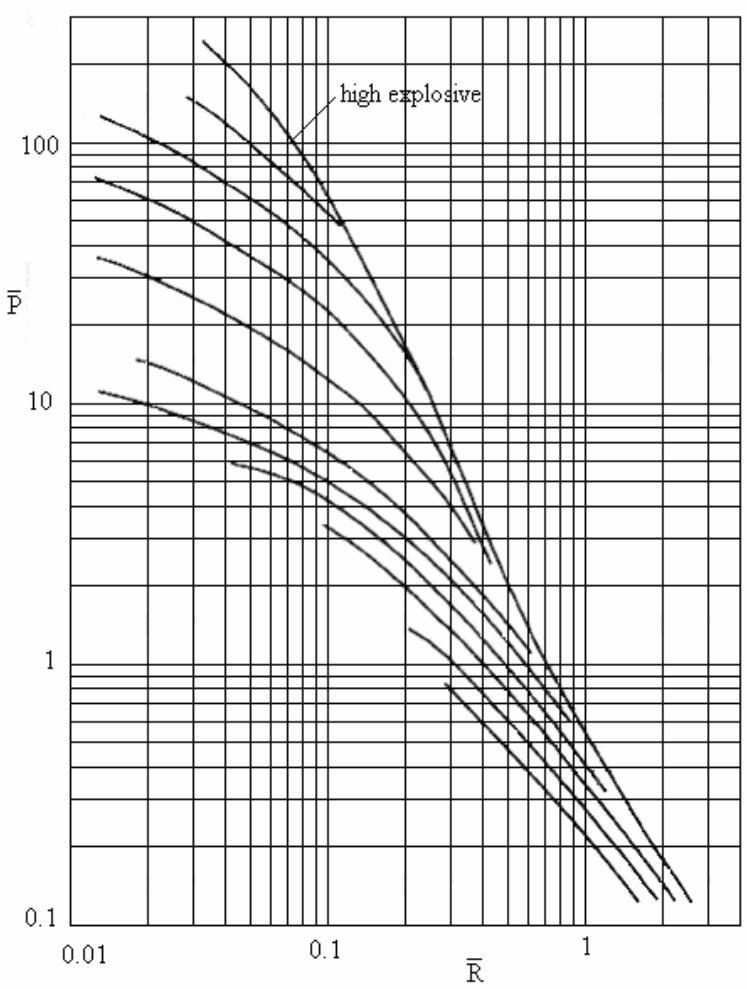

Fig. 4.2. Relative overpressure of shock wave $\overline{P}$ as function of relative distance $\overline{R}$ caused by a pressure vessel explosion according to Baker. $\overline{P} = p / p_a - 1$ [2].

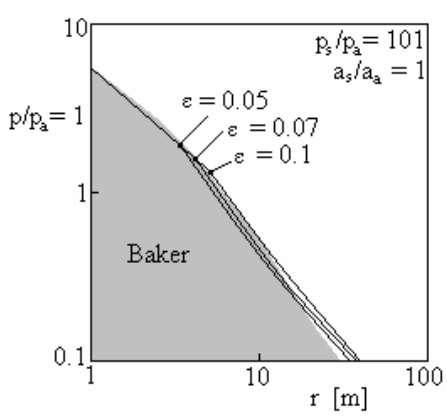

Fig. 4.3. Comparison with Baker's theory. The shock wave was caused by the burst of a hemispherical air vessel with 1 m radius. Baker's curve is coloured grey.
$p_s/pa - 1 = 100$, $a_s/a_a = 1$.

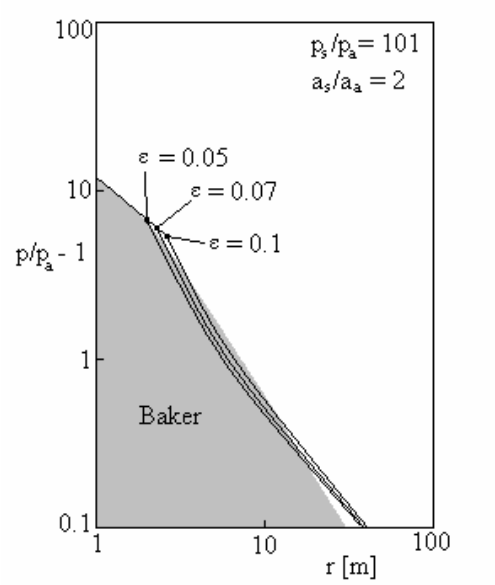

Fig. 4.4. Comparison with Baker's theory. The shock wave was caused by the burst of a hemispherical air vessel with 1 m radius. Baker's curve is painted with grey colour.
$p_s/pa - 1 = 100$, $a_s/a_a = 2$.

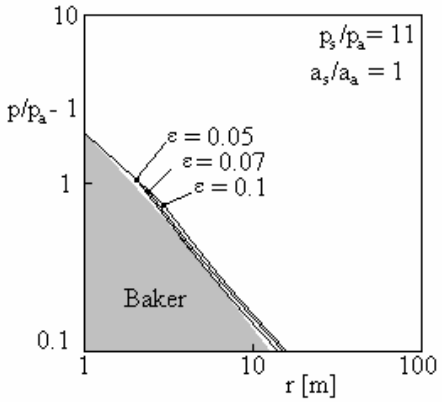

Fig. 4.5. Comparison with Baker's theory. The shock wave was caused by the burst of a hemispherical air vessel with 1 m radius. Baker's curve is painted with grey colour. $p_s/pa - 1 = 10$, $a_s/a_a = 1$.

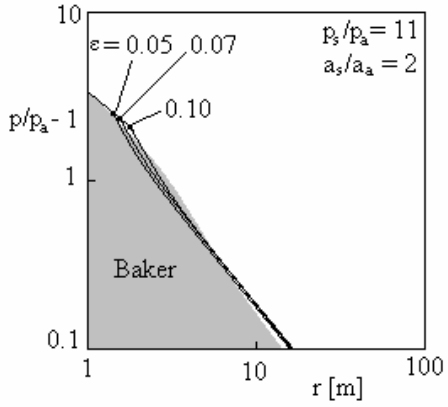

Fig. 4.6. Comparison with Baker's theory. The shock wave was caused by the burst of a hemispherical air vessel with 1 m radius. Baker's curve is painted with grey colour. $p_s/pa - 1 = 10$, $a_s/a_a = 2$.

It can be seen in figures 4.3, 4.4, 4.5 and 4.6 that $\varepsilon = 0.07$ is a satisfying estimation where the theory equals Baker's theory in the semi-sphere case. In this proposed theory, as well, a rough assumption can be made that the same ε-value ($\varepsilon = 0.07$) works in the other cases as in the spherical and cylindrical cases.

4.2.2 Comparison with a case of the GRP –method

The most advanced estimation method is the Generalized Riemann Problem method (GRP). With the GRP it is possible to estimate the distribution of density, flow velocity and pressure in the explosion process as functions of distance and time [4].

Saito and Glass (1984) have made a computational simulation on an example of an exploding helium sphere surrounded by air [25], where the basic data were: sphere radius r_s = 2.54 cm, pressure ratio p_s/p_a= 18.25, relative helium density ρ_s/ρ_a = 2.523, adiabatic factor of helium κ_s = 1.667, and ambient adiabatic factor κ_a = 1.4. The starting pressure ratio of the explosion was calculated as 6.497. The values of the theory were calculated as presented in chapter 4.1. The transition point was chosen with ε = 0.07.

The simulation results are presented in Figures 4.7 and 4.8. Comparison with the proposed theory is illustrated in Figure 4.9.

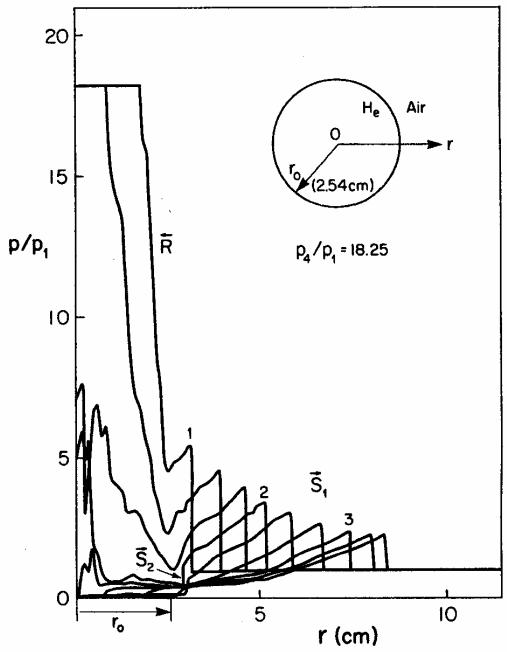

Fig. 4.7. First part of the results of a GRP-simulation with a helium bubble by Saito and Glass (1984) [25]. The pressure-distance profiles were simulated at different times.

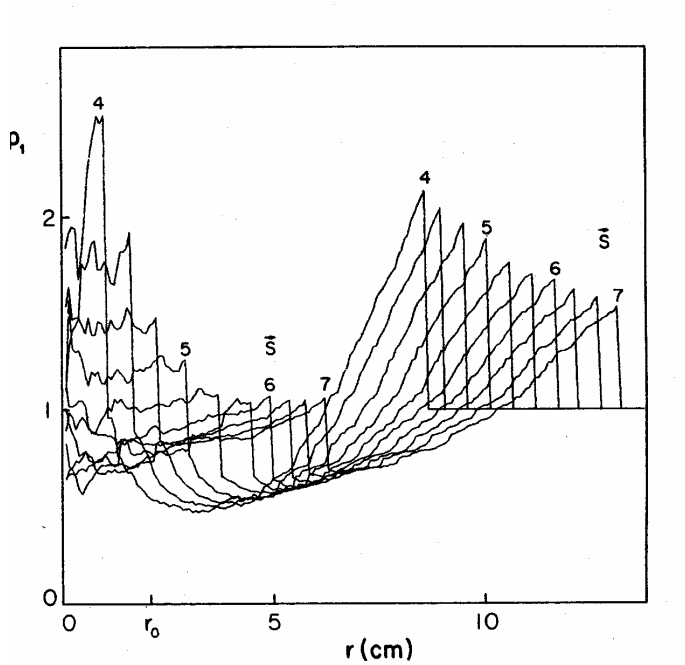

Fig 4.8. Second part of the results of a GRP-simulation with the helium bubble by Saito and Glass (1984) [25]. The pressure-distance profiles at different times were simulated.

The results of pressure and distance were measured graphically from Figure 4.7 and Figure 4.8. Only the main shock waves were taken into account. The results of the main shock wave are compared with the proposed theory in Figure 4.9.

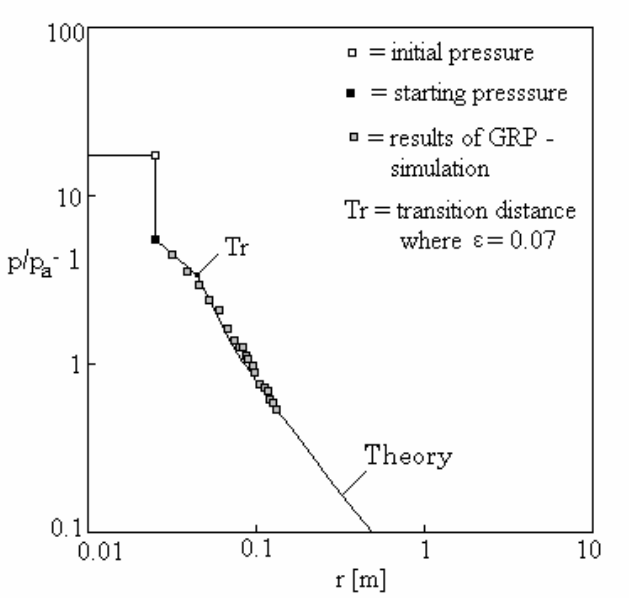

Fig. 4.9. Comparison of the proposed theory with the results of the GRP-simulation with the helium bubble by Saito and Glass (1984).

4.2.3 Application of ε-value into cylinders

A rough assumption is made that the value ε = 0.07 would be applicable also in the case of cylindrical pressure vessels. The transition distance in a cylindrical case seems to be much greater than in the corresponding hemispherical case, which is illustrated in Figure 4.10.

A transition point is situated on the shock wave curve in the simple state and its position on the curve depends on the ε –value. Alternative positions of the transition points and shock wave curves of the non-simple states are illustrated in a pr –diagram in Figure 4.11. It concerns a burst test carried out for a cylindrical pressure vessel [28]. The test was made by Langley et al. and will be discussed more closely in chapter 5.1.2.

In Figure 4.11 the positions of the transition points are compared to the test results. Five test points were measured. All the test points seem to be situated in the simple state. Figure 4.11 shows that the ε –value must be at least 0.04. On the other hand, when the ε –value grows close to 0.1, the problem loses its relevance because the curve of the non-simple state nears the curve of the simple state. Figure 4.11 shows that also the ε -value 0.07 is quite adequate.

The curves of the shock wave pressure as a function of the distance for five pressure vessels are presented in Figure 4.12. Each pressure vessel contains air with the ratio of burst overpressure 100 and volume 1 m^3. The sound velocity ratios are $a_a/a_s = 0.5$. The pressure vessel types are three cylinders L/D = 10, 5 and 2, one sphere and one hemisphere. (L = length of cylinder, D = diameter).

It can be noticed in Figure 4.12 that the position of the transition point depends on the shape of the pressure vessel. It can also be noticed that the longer and narrower the pressure vessel is, the farther the transition point is situated. In the case of long tubes the transition point is situated at an infinite distance and only the simple state becomes significant. The shock wave curves of the non-simple state are united at the distance when the initial values of the pressure vessels are similar, although the shapes differ.

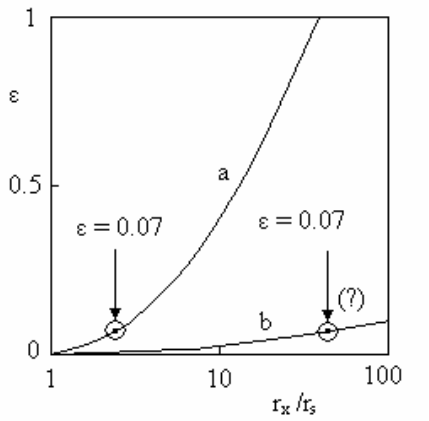

Fig. 4.10. Relative transition distance r_x/r_s as a function of isentropic exergy ratio ε. The shape of the pressure vessel is a) hemisphere, b) cylinder with L/D = 10. Points with ε = 0.07 are circled. L = length of the cylinder, D = diameter of the cylinder.

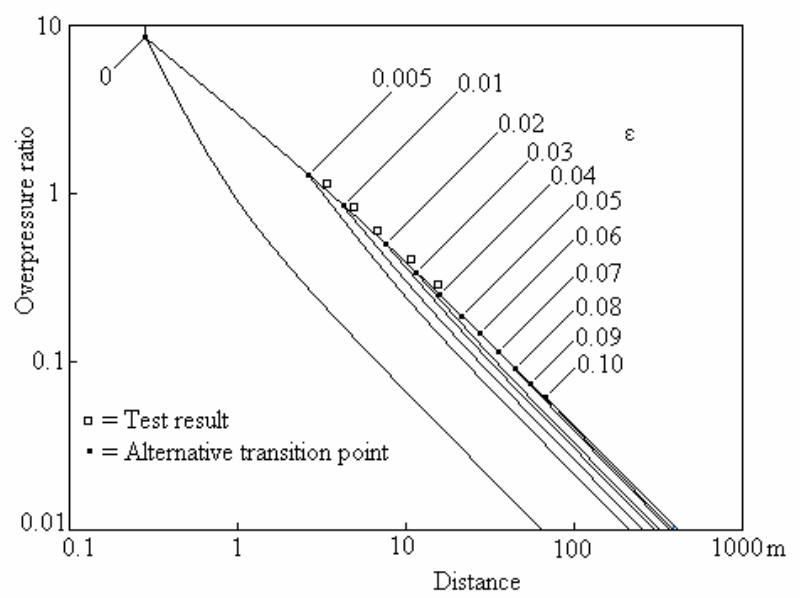

Fig 4.11. Positions of the transition points depending on the ε –values in the case of a burst test of a cylindrical pressure vessel done by Langley et al [28]. The points were set on the shock wave curve of the simple state defined by the test values. The alternative transition points and the shock wave curves in the non-simple states were compared with the test results.

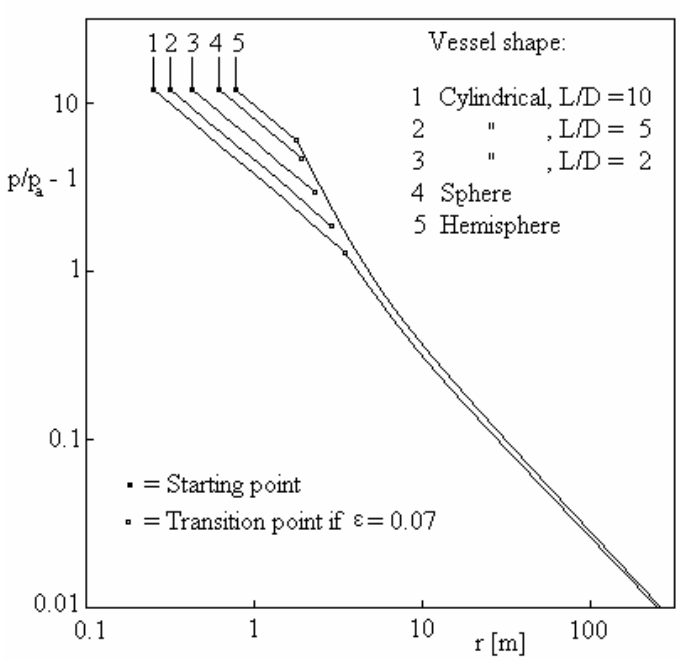

Fig. 4.12. Curves of shock wave pressure as a function of distance caused by bursts of five air containers having similar volumes and gas values. The volume $V_s = 1\ m^3$, burst overpressure ratio $p_s/p_a - 1 = 100$ and the ratio of the sound velocity $a_a/a_s = 0.5$.

5 Comparisons

5.1 Test results

5.1.1 Spherical pressure vessels

Seven spherical pressure vessels containing argon gas were made to burst by Pohto (1978) at pressures 15000 psi (103.4 MPa), 30000 psi (206.8 MPa) and 50000 psi (344.7 MPa) [27]. The test temperatures in the vessels were 17 ^{o}C (ambient temperature) and 1750 ^{o}C. The volume of the vessels was 29 litres and the inner radius was 190.5 mm. The vessels were situated in a concrete box as illustrated in Figure 5.1. The pressures of the main shock wave were measured at different distances and angles in the tests. The highest pressure values existed in the front of the open side of the box.

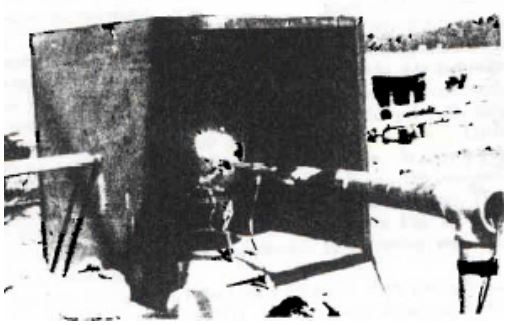

Fig. 5.1. Arrangement of the bursting tests made by Pohto (1978). The pressure vessel was situated in a concrete box. [27]

Six tests are discussed here. The chosen pressure results were measured in the front of the box opening.

The calculations according to the proposed theory concerning the test with overpressure 15000 psi (130.4 MPa) and ambient temperature 17 ^{o}C are presented. At first the ratio of sound velocity must be calculated. It is obtained from the equation:

$$a_a / a_s = \sqrt{\frac{\kappa_a R_a T_a}{\kappa_s R_s T_s}} \tag{5.1.1}$$

where

a_a/a_s = sound velocity ratio,

R_s = gas constant of argon = 208.2 J/kgK,

R_a = gas constant of air = 287.0 J/kgK,

κ_s = adiabatic factor of argon = 1.667,

κ_a = adiabatic factor of air = 1.4,

T_s = temperature of argon = 17 + 273.15 K,

T_a = ambient temperature = 17 +273.15 K.

By substituting the values into equation (5.1.1) we get:

$$a_a / a_s = \sqrt{\frac{1.4 \cdot 287.0 \cdot (17 + 273.15)}{1.667 \cdot 208 \cdot (17 + 273.15)}} = 1.076 \tag{5.1.1}$$

Secondly, the relative starting pressure of the shock wave must be calculated. It can be iterated from equation (2.4.7):

$$p_s = p_1 \left\{ 1 - \frac{a_a / a_s (\kappa_s - 1)(p_1 - p_a)}{\sqrt{2\kappa_a p_a [(\kappa_a + 1)p_1 + (\kappa_a - 1)p_a]}} \right\}^{\frac{-2\kappa_s}{\kappa_s - 1}} \tag{2.4.7}$$

where

p_s = burst pressure = 130.4 MPa (relative burst pressure = 1021),

p_1 = starting pressure of the shock wave,

p_a = ambient pressure = 0.101325 MPa (relative ambient pressure = 1).

By iteration from equation (2.4.7) we get the relative starting pressure, $p_1/p_a = 7.151$.

$$1021 = 7.151 \cdot \left\{ 1 - \frac{1{,}076 \cdot (1.667 - 1)(7.151 - 1)}{\sqrt{2 \cdot 1.4 \cdot [(1.4 + 1) \cdot 7.151 + (1.4 - 1)]}} \right\}^{\frac{-2 \cdot 1.667}{1.667 - 1}} \tag{2.4.7}$$

With the help of the starting pressure ratio, $p_1/p_a = 7.151$, the table distance of the starting point $R_{T1} = 31.69$ m and isentropic exergy $E_{T1}/p_a = 77987$ m^3 are obtained from the table in Appendix 2. The actual starting distance is the inner radius of the vessel, $r_s = 0.1905$ m. The overpressure ratio as a function of the distance in the simple state is obtained from Appendix table 2.

In order to define the transition point, the data of the isentropic exergy of the pressure vessel is needed. It is obtained from equation (2.1.7):

$$E = \frac{\kappa}{\kappa - 1} p_1 V_1 \left[1 - \left(\frac{p_a}{p_1} \right)^{\frac{\kappa - 1}{\kappa}} \right] - V_1 (p_1 - p_a) \tag{2.1.7}$$

where

p_1 = burst pressure of the vessel, which is the same as p_s here,

V_1 = volume of the pressure vessel = 0.02896 m^3.

By substituting the values into equation (2.1.7) we can get the relative value, E_s/p_a:

$$E_s / p_a = \frac{1.667}{1.667 - 1} \cdot 1021 \cdot 0.02896 \cdot \left[1 - \left(\frac{1}{1021} \right)^{\frac{1.667-1}{1.667}} \right] - 0.02896 \cdot (1021 - 1) = 39.76 \text{ m}^2 \tag{2.1.7}$$

The transition point can be obtained with the help of equation (4.1.3):

$$E_{Tx} / p_a = \left(\frac{R_{T1}}{r_s} \right)^3 \varepsilon E_s / p_a + E_{T1} / p_a \tag{4.1.3}$$

where

R_{T1} = table distance = 31.69 m,

r_s = radius of the pressure vessel = 0.1905 m,

E_{Tx}/p_a = loss of the isentropic exergy in the simple state,

E_{T1}/p_a = cumulative loss ratio of the isentropic exergy at the starting point from the table in Appendix 2, $E_{T1}/p_a = 77987\ m^3$,
ε = loss ratio of the isentropic exergy in the simple state, $\varepsilon = 0.07$,
E_s/p_a = isentropic exergy ratio of the pressure vessel, $E_s/p_a = 39.76\ m^3$.

By substituting the values into equation (4.1.3) we can obtain the table value of the isentropic exergy at the transition point:

$$E_{Tx}/p_a = \left(\frac{31.69}{0.1905}\right)^3 \cdot 0.07 \cdot 39.76 + 77987 = 12890260 \qquad (4.1.3)$$

With the help of the data $E_{Tx}/p_a = 23106213$, the corresponding pressure ratio $p_{Tx}/p_a = 1.2887$ and distance $R_{Tx} = 1016$ m can be obtained from the table in Appendix 2.

The real transition distance r_x can be obtained from equation (4.1.4):

$$r_x = \frac{R_{Tx}}{R_{T1}} r_s = \frac{1016}{31.69} \cdot 0.1905 = 6.105 \text{ m} \qquad (4.1.4)$$

After this it is necessary to produce the function of the non-simple state. In chapter 3.2.4, equation (3.2.10) was obtained:

$$\frac{(\kappa-1)p + (\kappa+1)p_a}{(\kappa+1)p + (\kappa-1)p_a}\left(\frac{p}{p_a}\right)^{\frac{1}{\kappa}} - 1 = \left[\frac{(\kappa-1)p_x + (\kappa+1)p_a}{(\kappa+1)p_x + (\kappa-1)p_a}\left(\frac{p_x}{p_a}\right)^{\frac{1}{\kappa}} - 1\right]\left(\frac{r}{r_x}\right)^{3n} \qquad (3.2.10)$$

Also equation (3.2.12) for the exponent n was obtained:

$$n = -\frac{\kappa}{\kappa-1}\frac{2\pi r_x^3}{3}\frac{p_a}{(1-\varepsilon)E_s}\left[\frac{(\kappa-1)p_x + (\kappa+1)p_a}{(\kappa+1)p_x + (\kappa-1)p_a}\left(\frac{p_x}{p_a}\right)^{\frac{1}{\kappa}} - 1\right] - 1 \qquad (3.2.12)$$

By substituting the values and by taking into account that κ = 1.4, the exponent can be calculated:

$$n = -\frac{7\cdot\pi\cdot 6.105^3}{3}\frac{1}{(1-0.07)\cdot 39.76}\left[\frac{1.2887+6}{6\cdot 1.2887+1}\cdot 1.2887^{\frac{1}{1.4}}-1\right]-1=-1.021 \tag{3.2.12}$$

The function can be calculated as follows:

$$\frac{p+6p_a}{6p+p_a}\left(\frac{p}{p_a}\right)^{\frac{1}{1.4}}-1=\left[\frac{1.2887+6}{6\cdot 1.2887+1}\cdot 1.2887^{\frac{1}{1.4}}-1\right]\left(\frac{r}{6.105}\right)^{-3\cdot 1.021} \tag{3.2.10}$$

By simplifying we get:

$$\frac{p/p_a+6}{6(p/p_a)+1}\left(\frac{p}{p_a}\right)^{\frac{1}{1.4}}-1=0.0004751\cdot\left(\frac{6.105}{r}\right)^{3.063} \tag{3.2.10}$$

In the same way as presented above, the tests in pressures 30000 psi (206.8 MPa) and 50000 psi (344.7 MPa) can be calculated. The starting values and the calculated values are as follows:

<u>30000 psi (206.8 MPa) ambient temperature:</u>

Ratio of sound velocity: $a_a/a_s = 1.076$

Burst pressure ratio: $p_s/p_a = 2042$

Ratio of the starting pressure of the shock wave: $p_1/p_a = 7.877$

Table value of the starting distance: $R_{T1} = 27.70$ m

Table value of the isentropic exergy loss at the starting point: $E_{T1}/p_a = 59416$ m^3

Isentropic exergy ratio of the pressure vessel: $E_s/p_a = 81.72$ m^3

Table value of the transition distance: $R_{Tx} = 1507$ m

Actual transition distance: $r_x = 10.36$ m

Ratio of the transition pressure: $p_x/p_a = 1.1983$

Exponent in the non-simple state: n = -1.019

50000 psi (344.7 MPa) ambient temperature:

Ratio of sound velocity: $a_a/a_s = 1.076$

Burst pressure ratio: $p_s/p_a = 3403$

Ratio of the starting pressure of the shock wave: $p_1/p_a = 8.391$

Table value of the starting distance: $R_{T1} = 25.44$ m

Table value of the isentropic exergy loss at the starting point: $E_{T1}/p_a = 50073$ m^3

Isentropic exergy ratio of the pressure vessel: $E_s/p_a = 138.32$ m^3

Table value of the transition distance: $R_{Tx} = 2230$ m

Actual transition distance: $r_x = 16.70$ m

Ratio of the transition pressure: $p_x/p_a = 1.1361$

Exponent in the non-simple state: $n = -1.019$

The test results and the calculated values according to the proposed theory are presented in Figure 5.2. Pohto has drawn all the three test results on one line because the results were so close to each other. The full line represents the measured results and the dotted line the evaluations. The figure reveals a notable difference between the results of the tests and the theory. Probably there is something wrong in the basic data because the starting pressure differs essentially from the theory. The equation (2.4.7) concerning the starting pressure of a shock wave is well known and it has also been applied in earlier theories.

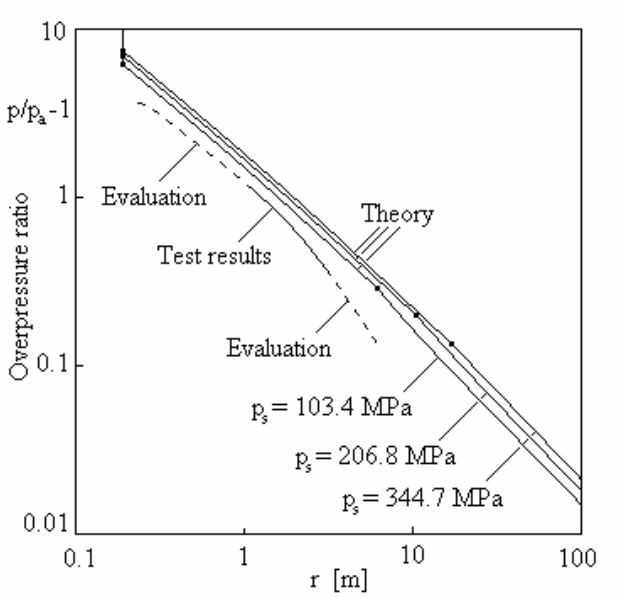

Fig 5.2. Comparison of the proposed theory with Pohto's burst test with argon gas at over-pressures 15000 psi (103.4 MPa), 30000 psi (206.8 MPa) and 50000 psi (344.7 MPa) and ambient temperature 17 ^{o}C. The complete line represents the measured results, the dotted lines the evaluations by the researcher.

Tests were also made with the burst temperature of 1750 ^{o}C in the pressure vessels. In this temperature, comparisons between the results of the tests and the proposed theory were made as above.

<u>15000 psi (103.4 MPa), 1750 ^{o}C:</u>

Ratio of sound velocity: $a_a/a_s = 0.4075$

Burst pressure ratio: $p_s/p_a = 1021$

Ratio of the starting pressure of the shock wave: $p_1/p_a = 26.55$

Table value of the starting distance: $R_{T1} = 5.537$ m

Table value of the isentropic exergy loss at the starting point: $E_{T1}/p_a = 1824$ m^3

Isentropic exergy ratio of the pressure vessel: $E_s/p_a = 39.76$ m^3

Table value of the transition distance: $R_{Tx} = 30.01$ m

Actual transition distance: $r_x = 1.032$ m

Ratio of the transition pressure: $p_x/p_a = 7.457$

Exponent in the non-simple state: $n = -1.081$

The results are presented in Figure 5.3.

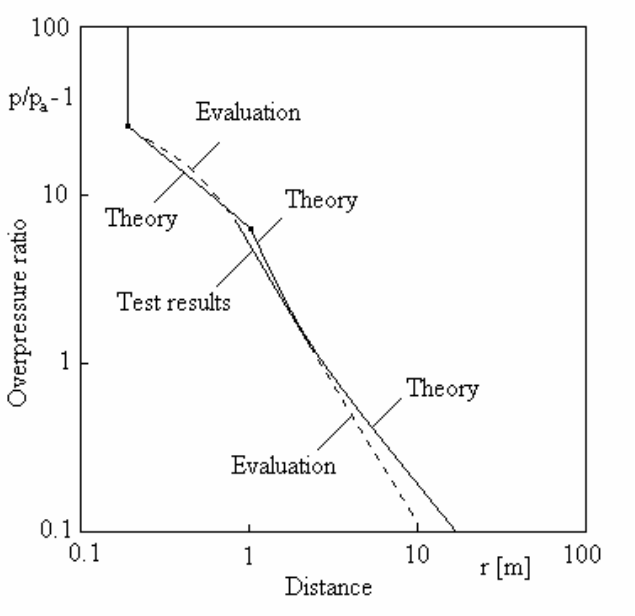

Fig. 5.3. Comparison of the proposed theory with Pohto's burst test with argon gas at pressure 15000 psig (103.4 MPa) and temperature 1750 ^{o}C. The complete line represents the measured results, the dotted lines the evaluations by the researcher.

<u>30000 psi (206.8 MPa), 1750 ^{o}C:</u>

Ratio of sound velocity: $a_a/a_s = 0.4075$

Burst pressure ratio: $p_s/p_a = 2042$

Ratio of the starting pressure of the shock wave: $p_1/p_a = 31.48$

Table value of the starting distance: $R_{T1} = 4.452$ m

Table value of the isentropic exergy loss at the starting point: $E_{T1}/p_a = 1104$ m^3

Isentropic exergy ratio of the pressure vessel: $E_s/p_a = 81.72$ m^3

Table value of the transition distance: $R_{Tx} = 30.86$ m

Actual transition distance: $r_x = 1.320$ m

Ratio of the transition pressure: $p_x/p_a = 7.302$

Exponent in the non-simple state: $n = -1.051$

The results are presented in Figure 5.4.

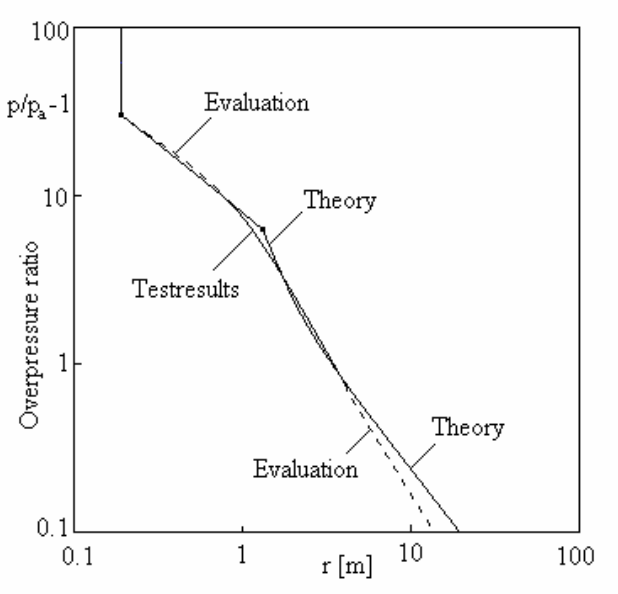

Fig. 5.4. Comparison of the proposed theory with Pohto's burst test with argon gas at pressure 30000 psig (206.8 MPa) and temperature 1750 ^{o}C. The complete line represents the measured results, the dotted lines the evaluations by the researcher.

50000 psi (344.7 MPa), 1750 ^{o}C:

Ratio of sound velocity: $a_a/a_s = 0.4075$

Burst pressure ratio: $p_s/p_a = 3403$

Ratio of the starting pressure of the shock wave: $p_1/p_a = 34.90$

Table value of the starting distance: $R_{T1} = 3.910$ m

Table value of the isentropic exergy loss at the starting point: $E_{T1}/p_a = 818.1$ m^3

Isentropic exergy ratio of the pressure vessel: $E_s/p_a = 138.32$ m^3

Table value of the transition distance: $R_{Tx} = 33.00$ m

Actual transition distance: $r_x = 1.608$ m

Ratio of the transition pressure: $p_x/p_a = 6.939$

Exponent in the non-simple state: $n = -1.050$

The results are presented in Figure 5.5.

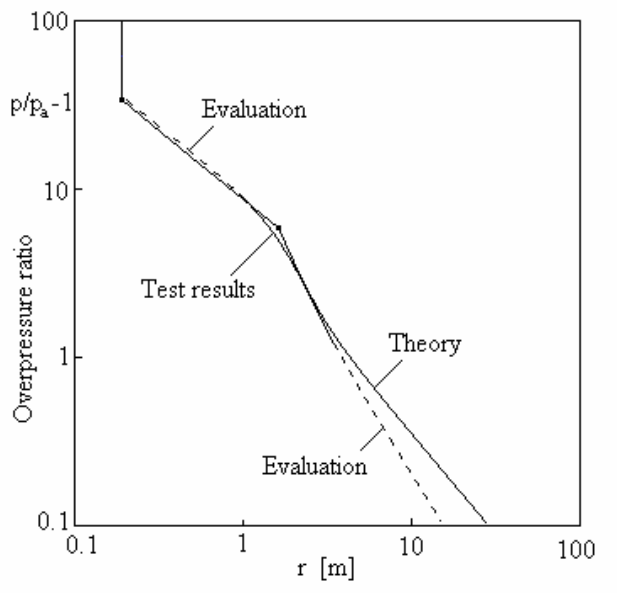

Fig. 5.5. Comparison of the proposed theory with Pohto's burst test with argon gas at pressure 50000 psig (344.3 MPa) and temperature 1750 ^{o}C. The complete line represents the measured results, the dotted lines the evaluations by the tester.

In the low values of the overpressure ratio (below 1), the theoretical results show higher values than those of the researcher. There are two possible reasons: Firstly, the tested pressure vessels were sited in a concrete box which probably caused a remarkable disturbance to the measurements. Strong reflected shock waves may have developed in the box walls, which may have decreased the isentropic exergy and the pressure of the main shock wave effectively. Secondly, in the low values of the overpressure the issued values were not measured, only evaluated.

5.1.2 Cylindrical pressure vessel

Langley et al. issued a commercial computer program PVHAZARD dealing with the risks of pressure vessel explosions in 1996 [28]. One of their aims was to test how well the program can evaluate the pressure of a shock wave as a function of distance. In that context Langley et al. have published the results of an explosion test of a pressure vessel.

The tested horizontal pressure vessel cylinder was sited on the ground. A large defect was made in the middle of the cylinder side. The vessel including nitrogen at ambient temperature was let burst by an overpressure. The shock wave pressures and impulses were measured at different distances and angles. A schematic test arrangement is presented in Figure 5.6.

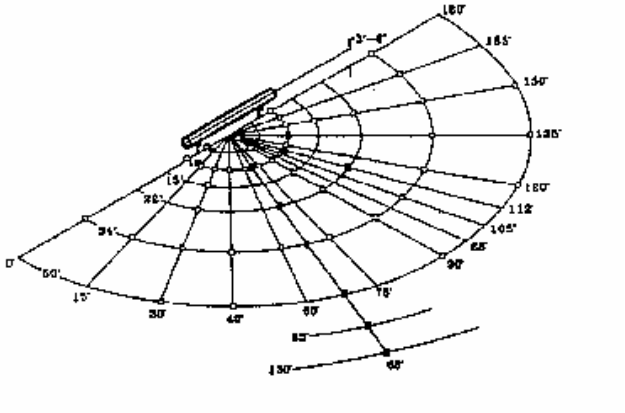

Fig. 5.6. Test arrangement of Langley et al. [28]

The initial values of the pressure vessel were:

Type of pressure vessel:	Longitudinal cylinder		
Content:	Nitrogen		
Pressure:	4700 PSIG	325 bar	$p_s/p_a = 320.8$
Gas temperature:	124 ^oF	51.11 ^oC	
Ambient temperature:	60 ^oF	15.56 ^oC	
Length of cylinder:	19 ft	5.79 m	
Inner radius of cylinder	0.93 ft	0.2835 m	

The maximum values of the shock wave pressure were obtained at normal angle, here 90^o.
The measured test results at 90^o angle were as follows:

Distance from the cylinder axis (m)	3.35	4.88	6.71	10.7	15.6
Ratio of overpressure $p/p_a - 1$	1.14	0.826	0.598	0.409	0.290

From the data of the pressure vessel, also the following can be obtained:

Volume of the pressure vessel,	V_s =1.5 m^3
Isentropic exergy ratio of the pressure vessel from equation (2.1.7)	E_s/p_a = 881 m^3
Gas constant of nitrogen	R_s = 296.8 J/kgK
Gas constant of air	R_a = 287.0 J/kgK
Adiabatic factor of nitrogen	κ_s = 1.4
Adiabatic factor of air	κ_a = 1.4

In order to define the starting pressure of the shock wave p_1, the ratio of sound velocity a_a/a_s must be obtained. Here a_a is the ambient sound velocity and a_s is the initial sound velocity in the pressure vessel gas. The ratio of sound velocity can be obtained from equation (5.1.1):

$$a_a/a_s = \sqrt{\frac{\kappa_a R_a T_a}{\kappa_s R_s T_s}} \tag{5.1.1}$$

where

T_s = initial gas temperature in the vessel, = 51.11 ^oC,

T_a = ambient temperature, = 15.56 ^oC.

By substitution we get:

$$a_a/a_s = \sqrt{\frac{1.4 \cdot 287.0 \cdot (15.56 + 273.15)}{1.4 \cdot 296.8 \cdot (51.11 + 273.15)}} = 0.9279 \tag{5.1.1}$$

The ratio of the starting pressure of the explosion can be obtained by iteration from equation (2.4.7):

$$p_s = p_1 \left\{ 1 - \frac{a_a / a_s (\kappa_s - 1)(p_1 - p_a)}{\sqrt{2\kappa_a p_a [(\kappa_a + 1)p_1 + (\kappa_a - 1)p_a]}} \right\}^{\frac{-2\kappa_s}{\kappa_s - 1}} \tag{2.4.7}$$

By substitution we get:

$$9.607 \cdot \left\{ 1 - \frac{0.9279 \cdot (1.4-1) \cdot (9.607-1)}{\sqrt{2 \cdot 1.4 \cdot 1 \left[(1.4+1) \cdot 9.607 + (1.4-1) \cdot 1 \right]}} \right\}^{\frac{-2 \cdot 1.4}{1.4-1}} = 320.8 \qquad (2.4.7)$$

By iterating from equation (2.4.7) the ratio of starting pressure can be obtained as p_1/p_a = 9.607. From the table in Appendix 2 the following values can be obtained with the starting pressure ratio 9.607 as starting distance R_{T1} = 21.14 m and loss of isentropic exergy ratio E_{T1}/p_a = 34113 m^3. The table value of loss of isentropic exergy ratio at the transition point E_{Tx}/p_a can be obtained from equation (4.1.3) as:

$$E_{Tx} / p_a = \left(\frac{R_{T1}}{r_1} \right)^3 \varepsilon E_s / p_a + E_{T1} / p_a \qquad (4.1.3)$$

where

ε is the ratio of the loss of isentropic exergy in the simple state (ε = 0.07).

By substituting the values into (4.1.3) we get:

$$E_{Tx} / p_a = \left(\frac{21.14}{0.305} \right)^3 \cdot 0.07 \cdot 881 + 34113 = 20568861 \text{ m}^3 \qquad (4.1.3)$$

From the table in Appendix 2 we get the values of the transition point with the help of E_{Tx}/p_a = 20568861 m^3 as pressure ratio p_{Tr}/p_a = 1.1613 and table distance R_{Tr} = 1869 m. The real transition distance can be obtained from equation (4.1.4):

$$r_x = \frac{R_{Tx}}{R_{T1}} r_s = \frac{1869}{21.14} \cdot 0.2835 = 25.06 \text{ m} \qquad (4.1.4)$$

Because all the test distances were below 25.06 m, there is no need to handle the non-simple state here. The proposed theory is compared with the test results and PVHAZARD-program in Figure 5.7.

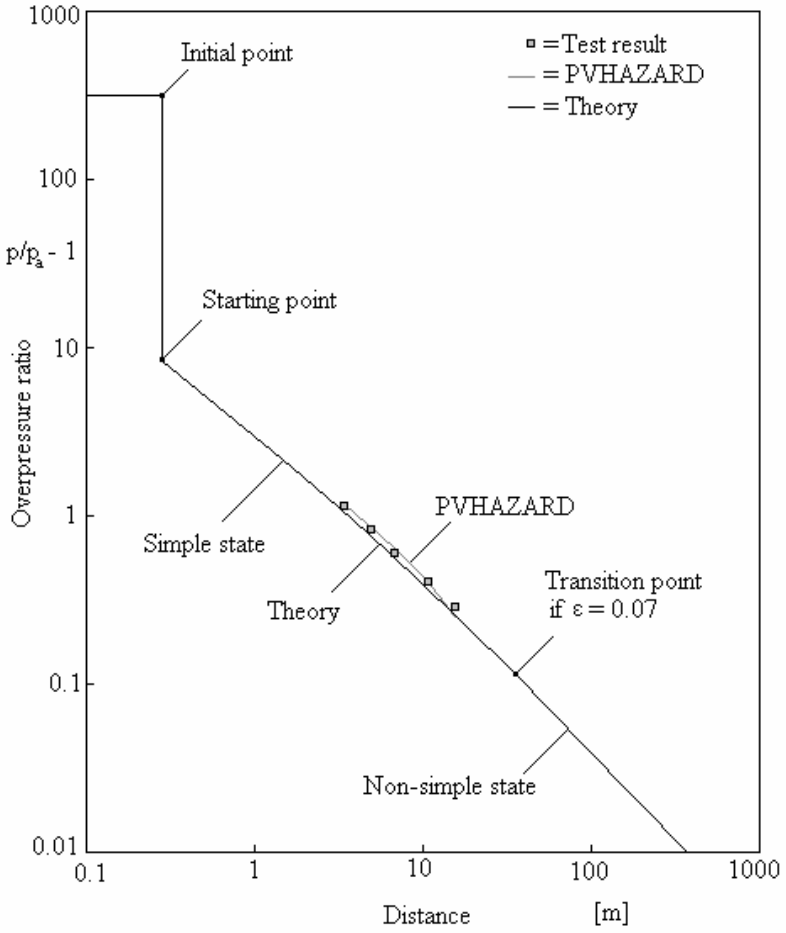

Fig. 5.7. Comparison of the test results of Langley et al. with the theory. The test results were measured at 90 ^{o} angle where the pressure values were the highest.

If $\varepsilon = 0.07$, the transition point moves outside the test range. Besides that, all the test points seem to be situated at the simple state. The test results do not negate the assumption that $\varepsilon = 0.07$ is applicable in a cylindrical case.

5.1.3 Tubes

Baum made tests on tube-shaped pressure vessels of steel in 1977 [26]. He made a long axial crack on the upper side of the cylinder wall. Causing an overpressure inside the vessels with air he broke them. By detectors at different distances above the pressure vessel he measured the pressure values of the shock wave. His aim was to study the effect of the velocity of the opening crack growth on the shock wave pressures. In his report Baum issued results of 7 tests. The pressure vessels contained air at ambient temperature. The test arrangement is illustrated in Figure 5.8.

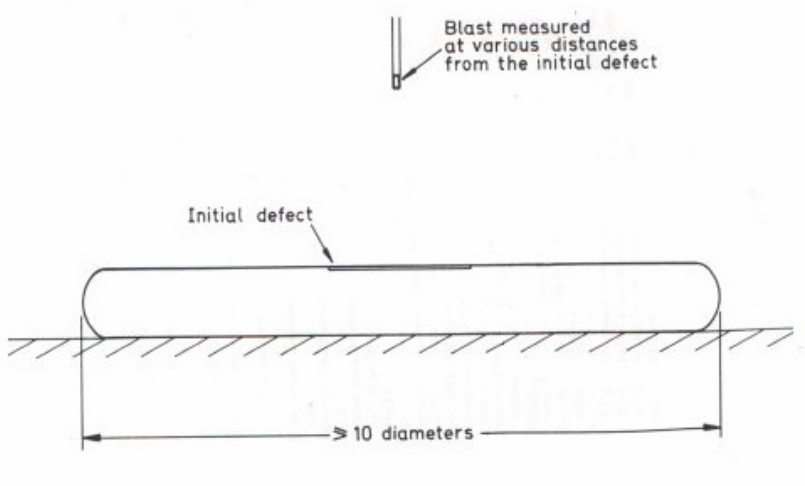

Fig 5.8. Baum's test arrangement [26]

The test results are presented below. The ratio of the starting pressure was calculated by the writer with equation (2.4.7). In this chapter the ambient pressure p_a is assumed to be 0.101325 MPa.

Test number 1

Pipe outside diameter (mm):	304		
Wall thickness (mm):	6		
Failure pressure (bars):	70		
Distance from detector (mm):	300	600	1200
Over-pressure of shock wave (bars):	4.6	4.1	0.7

Ratio of starting pressure from equation (2.4.7):	5.707			

Test number 2

Pipe outside diameter (mm):	152			
Wall thickness (mm):	6			
Failure pressure (bars):	92			
Distance from detector (mm):	150	300	2100	
Over-pressure of shock wave (bars):	5.2	3.7	0.22	
Ratio of starting pressure from equation (2.4.7):	6.210			

Test number 3

Pipe outside diameter (mm):	168			
Wall thickness (mm):	8			
Failure pressure (bars):	45			
Distance from detector (mm):	150	300	2100	
Over-pressure of shock wave (bars):	3.4	1.3	0.2	
Ratio of starting pressure from equation (2.4.7):	4.944			

Test number 4

Pipe outside diameter (mm):	152			
Wall thickness (mm):	6			
Failure pressure (bars):	46.3			
Distance from detector (mm):	150	300	450	1400
Over-pressure of shock wave (bars):	2.2	1.3	0.4	2.2
Ratio of starting pressure from equation (2.4.7):	5.991			

Test number 5

Pipe outside diameter (mm):	152
Wall thickness (mm):	6
Failure pressure (bars):	92.6
Distance from detector (mm):	600
Over-pressure of shock wave (bars):	1.45

Ratio of starting pressure from equation (2.4.7): 6.222

Test number 6

Pipe outside diameter (mm):	101
Wall thickness (mm):	1.6
Failure pressure (bars):	48.3
Distance from detector (mm):	340
Over-pressure of shock wave (bars):	2.0
Ratio of starting pressure from equation (2.4.7):	5.062

Test number 7

Pipe outside diameter (mm):	101
Wall thickness (mm):	1.6
Failure pressure (bars):	38.6
Distance from detector (mm):	340
Over-pressure of shock wave (bars):	2.0
Ratio of starting pressure from equation (2.4.7):	4.694

Baum did not express the exact volumes of the cylinders, and the cylinders were relatively long. The transition points were in the distance. That is why the test results are observed in the simple state only. The test results are presented in Figure 5.9, where the ratio of the overpressure p/p_a -1 and the distance of a detector for the cylinder axis r are stated. The test results are compared to the function in the simple state. Because in the simple state the shape of the function is permanent in all dimensions, the test results can be presented in the same figure. The starting points for the tests were chosen so that the points meet the actual starting pressure from the illustrated function.

A very interesting phenomenon can be discovered in Figure 5.9. In the beginning the pressure values of the main shock waves seem to be much higher than the function implies. The interesting behaviour may be caused by the relatively slow opening of the explosion slot. There may exist a jet flow outside the opening, and the cross section of its flow does not expand as much as the function distance implies. Later, the pressure values seem to become below the values of the function. The reason may be that the flow begins to reach the

hemispherically symmetric shape. At the transition region the type of the flow changes from jet to hemispherically symmetric. Then the flow may become wrinkled so that the flow cross section of the shock wave is temporarily larger than the function distance implies. Finally the pressure values seem to get close to the function.

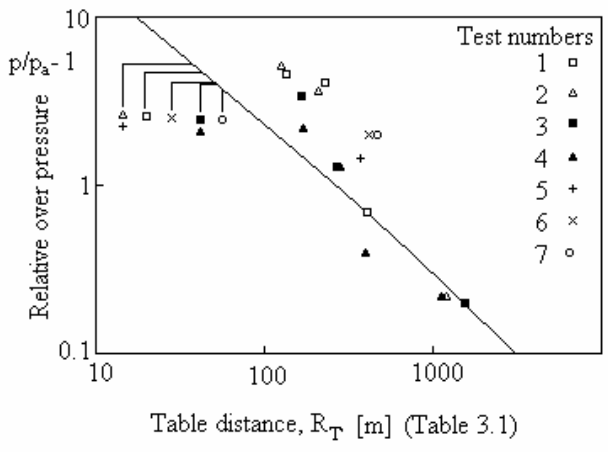

Fig. 5.9. Baum's test results collected in the same function of the simple state. The relative distance was chosen so that each test result meets the function at its starting pressure.

5.2 Accident analysis

5.2.1 Explosion of a steam generator of 150 litres

In February 1991 a steam generator exploded in a microbiology laboratory in Helsinki [30]. The volume of the generator was 150 litres and the highest allowed overpressure was 3 bars. The generator contained water in liquid and steam phases, 75 litres of each, in saturated states. The generator was heated by electricity and it produced steam for a sterilizing autoclave.

The reason for the accident was the contactor of the electric pressostat, which failed so that the overpressure rose to 30…40 bar, when the highest allowed overpressure was 3 bar. The safety valve failed as well. The isentropic exergy was evaluated to be 6 MJ.

The straight end of the generator came off and was thrown towards the external wall, which expanded. The generator collapsed towards an elevator shaft behind it which was broken. The shock wave pressure lifted the second floor of the building so that all the vertical tubes in the

room were cut off. A total chaos took place in the room. Doors and panels collapsed to the lobby, fourteen windows were broken, etc. Two persons in the lobby went into shock and were taken to a hospital. Fortunately nobody was present in the room and no casualties occurred. The consequences of the accident from one view are presented in Figure 5.10.

Let us observe the explosion accident with the proposed theory. At first the basic data must be defined:

Inner radius of the vessel:	$r_s = 0.225$ m
Burst pressure:	$p_s = 3.1$ MPa, $p_s/p_a = 30.59$
Adiabatic factor of the steam:	$\kappa_s = 1.319$ [23]
Density of the steam:	$\rho_s = 15.50$ kg/m^3
Isentropic exergy:	$E_s = 6$ MJ,
Air temperature in the room:	$T_a = 20$ ^{o}C,
Gas constant of air:	$R_a = 287$ J/kgK [23]
Adiabatic factor of air:	$\kappa_a = 1.4$

The ratio of the sound velocities is obtained from:

$$a_a / a_s = \sqrt{\frac{\kappa_a R_a T_a \rho_s}{\kappa_s p_s}} = \sqrt{\frac{1.4 \cdot 287 \cdot (20 + 273.15) \cdot 15.50}{1.319 \cdot 3.1 \cdot 10^6}} = 0.668 \qquad (5.2.1)$$

The starting point p_1 is obtained from equation (2.4.7):

$$p_s = p_1 \left\{ 1 - \frac{a_a / a_s (\kappa_s - 1)(p_1 - p_a)}{\sqrt{2\kappa p_a [(\kappa + 1) p_1 + (\kappa - 1) p_a]}} \right\}^{\frac{-2\kappa_s}{\kappa_s - 1}} \qquad (2.4.7)$$

Fig. 5.10. The lobby of the laboratory after the explosion of a steam generator, which occurred in the room in the back. The isentropic exergy was about 6 MJ [30].

By substituting the values into equation (2.4.7) we get:

$$30.59 = 6.375\left\{1 - \frac{0.668(1.319-1)(6.375-1)}{\sqrt{2\cdot 1.4\cdot 1\cdot\left[(1.4+1)6.375+(1.4-1)\cdot 1\right]}}\right\}^{\frac{-2\cdot 1.319_s}{1.319-1}} \qquad (2.4.7)$$

The starting pressure ratio is obtained as $p_1/p_a = 6.375$. The dimensions of the room were about 5x5x3 m^3, where the height was about 3 meters. The distances from the ceiling and the

walls to the pressure vessel were 2…4 meters. The transition distance is obtained as 8 meters. So the observed region is in the simple state only. The results obtained from Appendix table 2 are shown in the calculated data below and in Figure 5.11.

Starting distance in the table:	R_{T1} = 37.48 m, p_1/p_a = 6.375,
Loss of the isentropic exergy per ambient pressure at the starting point in the table:	E_{T1}/p_a = 109506 m^3
Isentropic exergy:	E_s/p_a = 59.2 m^3
Loss of the isentropic exergy per ambient pressure at the simple region in the table:	E_{Tx}/p_a = 16027270 m^3
Transition distance in the table:	R_{Tx} = 1701 m
Transition distance:	r_x = 10.21 m
Transition pressure ratio:	p_x/p_a = 1.1765
Exponent:	n = -1.0177

Stephens (1970) has described four damage level zones based on the overpressure of the main shock wave [2]:

> 83 kPa:	Total destruction. A building is totally destroyed if it is damaged beyond economical repair.
> 35 kPa:	Severe damage suggests partial collapse or failure of some bearing members.
> 17 kPa:	Moderate damage. A building is still usable, but structural repairs are required.
> 3.5 kPa:	Light damage: Consists of shattered window panes, light cracks in walls, and damage to wall panels and roofs.

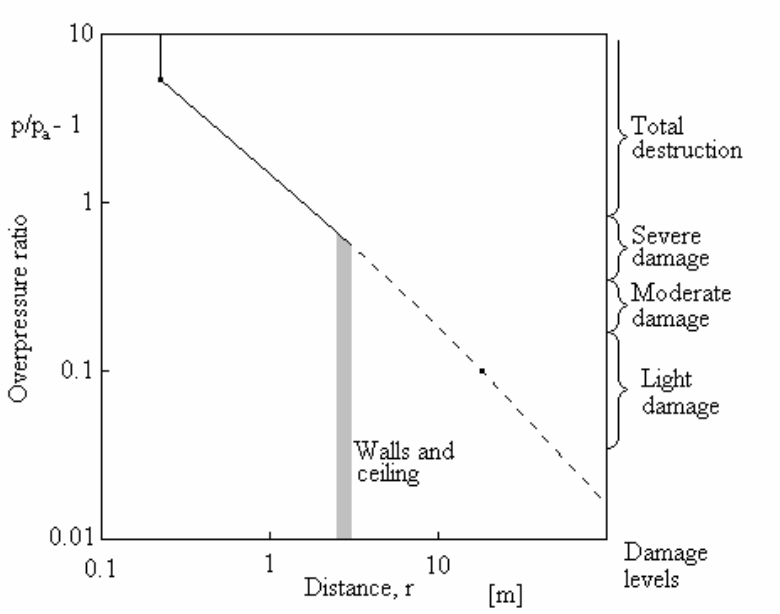

Fig. 5.11. Comparison of the proposed theory with the findings in the accident investigation and with the issued damage zones.

5.2.2 Explosion of a steam accumulator of 10 m^3

In February 1993 a pressure vessel explosion accident occurred at a plastic box factory in the village of Muurla in Southern Finland [31]. The pressure vessel was a steam accumulator with the volume of 10 m^3, placed inside a boiler house. In the explosion the boiler house was completely destroyed. The shock wave penetrated into the production building next to the boiler house and caused damages in it by moving walls, throwing objects, breaking down the lights etc. Parts of the windows and wall panels were thrown to the nearby road. Moreover, the shock wave ruined the nearby corner of the storage wing. A map and a view from the accident place are presented in Figures 5.12, 5.13 and 5.14.

The accumulator was broken in three pieces. A half of the vessel was thrown about 15 m behind the store building. The shell part was thrown 25 m towards the transformer building. One end was left in the ruins of the boiler house.

The reason for the accident was corrosion fatigue. It was a consequence of variable pressure in a corrosive environment, such as water. The explosion occurred seventeen minutes before

the working day would have begun. Fortunately nobody was present and no human casualties occurred. Neighbouring private houses are at about 200 m distance from the burst vessel but no damages occured. Even the windows remained unbroken.

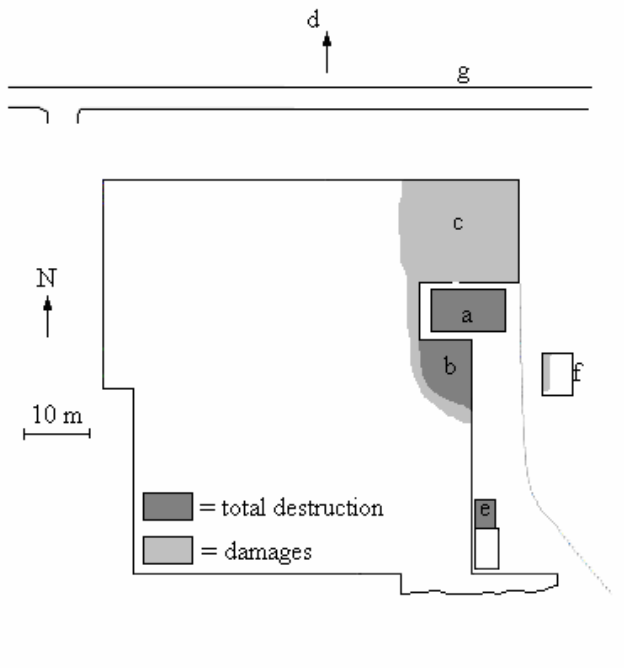

Fig. 5.12. Map over the accident area [31].
a) The destroyed boiler house. The starting point of the explosion was here.
b) A corner of the storage wing collapsed
c) The shock wave rushed in the production room causing damages.
d) Neighbours at 200 m distance were saved without damages.
e) The cylinder part of the vessel was thrown towards to a transformator.
f) A half of the vessel was thrown behind a storage building.
g) Pieces were flown to the road distance.

Fig. 5.13. View from the south direction [31]. The destroyed boiler house with the declined chimney is on the background. The collapsed storage wing is on the left.

The basic data of the burst accumulator are:

Volume:	$V_s = 10\ m^3$
Water volume:	$7.5\ m^3$
Steam volume:	$2.5\ m^3$
Inner radius:	$r_s = 0.99$ m
The highest allowed overpressure:	1 MPa
Assumed explosion overpressure:	$p_s = 0.7$ MPa
Assumed isentropic exergy:	$E_s = 150$ MJ

Fig 5.14. View from the same direction as in Fig. 5.13. The people give the scale [31].

The following values of the saturated steam can be obtained:

Adiabatic factor:	$\kappa_s = 1.324$ [23]
Pressure ratio:	$p_s/p_a = 7.895$
Density:	$\rho_s = 4.161$ kg/m^3
Sound velocity:	$a_s = 504.4$ m/s
Ambient sound velocity:	$a_a = 343.2$ m/s
Ratio of sound velocity:	$a_a/a_s = 0.680$

Ratio of starting pressure
of the shock wave: $p_1/p_a = 3.242$
Isentropic exergy per
ambient pressure: $E/p_a = 1500\ m^3$,
Starting distance in the table: $R_{T1} = 104.2$ m,
Starting ratio of isentropic exergy
in the table of Appendix 2 $E_{T1}/p_a = 702200\ m^3$,
Transition energy in the table: $E_{Tx}/p_a > 71360000$ (out of range).

As the transition point went out of the range of the observed region, the shock wave is illustrated in the simple state. The findings are compared with the theory in Figure 5.15. Also the effects of the shock wave pressure according to the literature [2] are compared.

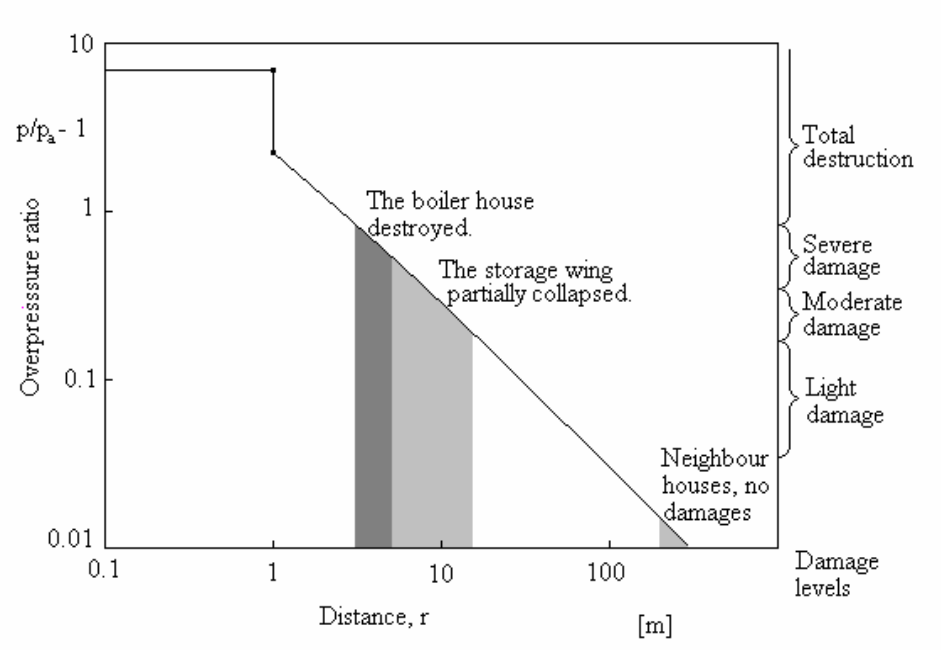

Fig. 5.1. Findings compared with the theory

The damages in the buildings seemed to be greater than the proposed method implies. The reason may be that the structures of the buildings were lighter than average.

6 Discussion

The destructive impacts of a pressure vessel burst or explosion can best be described by isentropic exergy. It differs from complete exergy so that the process of pressure drop into the ambient pressure is essentially isentropic. Usually the post-process temperature differs from the ambient one. That is why the value of isentropic exergy is usually smaller than that of complete exergy. The values are similar just in the special case when the post-process temperature is the same as the ambient one. In that case the entropy of the system is also the same as in its complete equilibrium state with the environment.

Although the word "isentropic exergy" seems to be new, the idea itself is well known especially in the field of thermodynamics. Baum has applied this idea for defining the explosion energy of pressure vessels.

The advantages of the concept of isentropic exergy are the following:

1) It describes the released energy of an explosion process in contrast to the increase in internal energy caused by pressurization.

2) It is in harmony with the second law of thermodynamics in contrast to the work specification.

3) It describes the fast nature of explosion without essential heat transfer in contrast to the exergy.

4) It can be applied to many thermodynamic systems with a batch process.

5) Its changes can be defined in a shock wave.

6) It offers a possibility to make a simple method for evaluating the shock wave pressure as a function of the distance caused by a pressure vessel explosion. This method is applicable to all shapes of pressure vessels in general use in contrast to the other theories.

The shock wave system is developed in an explosion process. The system contains the pressure vessel contents and the ambient gas. In the explosion process the developing shock wave system gets the initial isentropic exergy from the pressure vessel. Immediately after the start of the explosion process the shock wave system begins to lose its isentropic exergy. The losses are caused by the increase of the entropy in the shock fronts. In the end, the shock wave system has lost all of its isentropic exergy and the process is over.

In the shock tube theory it was noticed that the shock wave has a dual nature. At first the shock wave is in the simple state where its pressure is constant. When meeting the reflected

rarefaction wave, the type of the shock wave changes into a non-simple state when its pressure begins to decrease. The meeting point of the waves can be called the transition point and it separates the mentioned states. It was proved here that a similar dual nature exists also in hemispherically symmetric shock waves.

The proposed method for evaluating the shock wave pressure as a function of distance caused by a pressure vessel placed on land was developed. Equations concerning the changes of the isentropic exergy caused by a shock wave were derived. In the estimations, only the main shock wave was taken into account. The other existing shock waves were neglected. This principle gives a small over-estimation and therefore the theory is conservative. The method gives the highest estimation of the shock wave pressure at some distance.

The method presented in this study contains some assumptions and limitations:

1) The exploding pressure vessel is placed on the ground.

2) The ruptured opening area of the pressure vessel is fully open already at the beginning of the explosion process. This approximation repairs itself at a distance.

3) There exist no missiles, the shock wave only. The mass of the pressure vessel walls is neglected.

4) The shape of the shock wave is hemispherically symmetric. Although the shock wave is usually highly directional in the pressure vessel explosion, the estimation of hemispherical symmetry simulates the situation in front of the ruptured opening. Particularly this is the fact at a distance from the pressure vessel. Test results prove this argument.

6) The explosion is idealized so that all the losses of the isentropic exergy take place in the main shock front. The change processes are isentropic except in the main shock front. Chemical reactions and heat transfer are neglected. There are no ambient structures or destructions. Reflected shock waves are not assumed.

7) At the beginning of the explosion process the shock wave system is in the simple state. Then equation (3.1.57) or the table in Appendix 2 is applied. In the simple state the inner radius of the pressure vessel cylinder, the starting pressure of the shock wave and the distance are significant, but not the isentropic exergy.

8) Later the shock wave system is in the non-simple state. Then equations (3.2.10) and (3.2.12) are applied. The shock wave pressure in the non-simple state seems to be too complicated to handle analytically. On the other hand, the application of the idea of isentropic exergy is interesting. That is why equations (3.2.10) and (3.2.12) are derived with the self

similarity principle. In the non-simple state the isentropic exergy, the values in the transition point, and the distance are significant.

9) The transition point between the states is defined so that 7 percent of the initial isentropic exergy of the pressure vessel is lost in the simple state. Here the table in Appendix 2 was applied.

Several assumptions have been made in the method. Many of them are quite rough but the test results support these assumptions moderately at least at a distance. It is worth noting that the most interesting overpressure levels of the shock wave are about 1…10 kPa. These are the normal levels of the construction pressure in building structures. Normally, such pressures of a shock wave exist at the distances where this method gives its best estimations.

The innovations presented in this study are the following:

1) Isentropic exergy was discovered as explosion energy of a pressure vessel and its values were calculated.

2) Isentropic exergy was discovered to be an essential property of a shock wave system.

3) Equations concerning the loss of isentropic exergy in shock waves were derived.

4) Equations concerning shock wave pressure as a function of distance in the simple and the non-simple states were derived. The derivations were carried out with thermodynamics, flow theories and the concept of isentropic exergy.

5) A proposed method for calculating the shock wave pressure as a function of distance caused by an explosion of a pressure vessel was presented. The method is applicable for pressure vessels in all shapes in general use.

The proposed theory was compared with the results of three test series and the findings in two accident investigations. The comparisons confirm the results, or they do not contradict them.

Isentropic exergy is an essential safety property of a pressure vessel. Furthermore, it gives a new viewpoint and possibility for evaluating the pressure of a shock wave. It enables also an improved evaluation of the explosion risks in pressure vessels.

7 Conclusions

The concept of isentropic exergy offers a new perspective for evaluating the pressure of the shock wave caused by a pressure vessel explosion as a function of distance. The isentropic exergy in a pressure vessel and its losses in a shock wave, as well, can be calculated. The evaluations of the shock wave pressure as a function the distance can be carried out for pressure vessels in any shape in practical use.

There is a need for further studies to make this theory more precise and applicable, e.g. in the cases where the opening of the defect is taken into account or where the shock wave is highly directional. Also, pressure vessels with contents in two-phase state remain to be further studied.

8 References

1 Wees R. M. M., Mercx, W. P. M. and Weerheijm, J. Critical Appraisal of Damage Criteria for Buildings and Process Equipment. The First World Seminar on the Explosion Phenomenon and Application of Explosion Protection Techniques in Practice. Brussels, 1992.

2 Guidelines for Evaluating the Characteristics of Vapor Cloud Explosions, Flash Fires, and BLEVEs. American Institute of Chemical Engineers. Second printing. New York, 1998.

3 Ryti, H. Termodynamiikka. Tekniikan käsikirja 2. 3. painos. K. J. Gummerus Oy. Jyväskylä, 1973.

4 Falcovitz, J., Ben-Artzi, M. Recent Developments of the GRP Method. JSME, International Journal. Series B. Volume 38, No. 4, 1995, pp. 497-516.

5 Kinney, G. F., Explosive Shocks in Air. Second edition. Macmillan Company, New York, 1962.

6 Lee J. F, Sears F.W. Thermodynamics. An Introductory Text for Engineering Students. Addison- Wesley Publishing Company Inc. Second edition. Reading, Massachusetts, 1963.

7 Moran M.J, Shapiro H.N. Fundamentals of Engineering Thermodynamics. Second edition. John Wiley & Sons, Inc, New York, 1993.

8 Lees, Frank P. Loss Prevention in the Process Industries. Volume 1. Butterworth & Co Ltd, London, 1980. P. 565.

9 The Effects of Explosions in the Process Industries. First Paper of the Major Hazard Assessment Panel-Overpressure Working Party. Overpressure Monograph. Published by The Institution of Chemical Engineers. Rugby 1989. Reprinted 1990.

10 Kielec, D. J, Birk A.M. Analysis of Fire-Induced Ruptures of 400-l Propane Tanks. Transaction of ASME, Journal of Pressure Vessel Technology. August 1997, vol. 119, pp. 365-373.

11 Vanderstraeten, B., Boesmans, B. and Berghmans, J. Explosion energy of compressed gases at elevated temperatures. Loss Prevention and Safety Promotion in the Process Industries. Volume 2. Elsevier Science 1995, pp. 133-144.

12 Crowl, D. A. Calculating the Energy of Explosion Using Thermodynamic Availability. Journal of Loss Prevention in Process Industries. Volume 5, no 2, 1992, pp.109-118.

13 Baum, M. R. The Velocity of Missiles Generated by the Disintegration of Gas-Pressurised Vessels and Pipes. Central Electricity Generating Board. Technology Planning and Research Division. Berkeley Nuclear Laboratories. March 1983.

14 Baum, M. R. Disruptive failure of pressure vessels: Preliminary Design Guidelines for Fragment Velocity and the Extent of the Hazard Zone. Transactions of the ASME, Journal of Pressure Vessel Technology. May 1988, vol. 110, pp. 168 – 176.

15 Fullard K, Baum M.R, Barr P. The Assessment of Impact on Nuclear Power Plant Structures in the United Kingdom. Nuclear Engineering and Design. No 130, 1991, pp. 113 -120.

16 Kurttila, H. Energy and Impacts of Pressure Vessel Explosions. 25th MPA-Seminar October 7 and 8, 1999: Safety and Reliability of Plant Technology. (MPA), Stuttgart, 1999.

17 CRC Handbook of Chemistry and Physics. 55 th edition 1974-1975. CRC Press, Ohio 1975. P. F-5.

18 Perry's Chemical Engineers Handbook. Sixth edition. Mc Graw-Hill Book Company, Kosaido, Japan, 1984. Pp, 3-170, 3-217.

19 VDI – Wasserdamphtafeln. Mitt einem Mollier (h,s) Diagramm bis 800 ^{o}C und einem T,s –Diagramm. Sechste Auflage. Auslage B (Joule, bar). Springer-Verlag, Berlin 1963.

20 Yahya, S. M. Fundamentals of compressible flow. Wiley Eastern Limited. New Delhi. 1982.

21 Anderson, John D. Junior. Modern Compressible Flow with Historical Perspective. Second edition, McGraw-Hill, Inc, New York 1990. Pp. 206-241.

22 Lord Rayleigh. Aerial Plane Waves of Finite Amplitude. Proceedings of Royal Society, 1910, pp. 247 – 284.

23 Nashchokin, V. V. Engineering thermodynamics and heat transfer. MIR Publishers Moscow, 1975, English translation, 1979, pp. 141 – 142.

24a Barenblatt, G. I. Scaling, Self-Similarity, and Intermediate Asymptotics. Cambridge University Press 1996.

24b Barenblatt: Scaling Phenomena in Fluid Mechanics. Cambridge University Press. January 1995.

25 Saito, T. and Glass, I. I. Application of Random-Choice Method to Problems in Gas Dynamics. Progress in Aerospace Sciences. Vol. 21, no 3, 1984, pp. 201-247.

26 Baum, M. R. Blast waves generated by the rupture of gas pressurised ductile pipes. Trans IChemE, Vol. 57, Institution of Chemical Engineers.1979, pp. 15 – 24.

27 Pohto, H. A. Energy Release from Rupturing High-Pressure Vessels: A Possible Code Consideration. Transaction of ASME, Journal of Pressure Vessel Technology, May 1979 Vol. 101, pp. 165 – 170.

28 Langley, D. R., Chrostowski, J. D., Goldstein, S. and Cain, M. Pressure Vessel Burst Program. Automated Hazard Analysis for Pressure Vessels. PVP-Vol. 325, Structures Under Extreme Loading Conditions, ASME 1996, pp. 163 – 184.

29 Mathcad 2001 User's Guide with Reference Manual. MathSoft Engineering & Education, Inc. Cambridge, USA, February 2001.

30 Sterilointiautoklaavin höyrynkehittimen räjähdys Helsingin yliopiston biotekniikan laboratoriossa 12.2.1991. Tutkimusselostus. Teknillinen tarkastuskeskus, Helsinki, 1991.

31 Höyrynvaraajan räjähdys Yhtyneet paperitehtaat Oy Walki-Pakkauksen muovitehtaalla Muurlassa. Tutkimusselostus. Teknillinen tarkastuskeskus, Helsinki, 1993.

Appendix 1

Transition point in a shock tube

In this appendix the position of the transition point in a shock tube is derived. The purpose is to find simple conformity to the law of the shock tube theory, as a constant value. In a transition point the type of the shock wave transforms from a simple state into a non-simple state. In the simple state the pressure and the velocity of the shock wave are constant. At the non-simple state the values decrease. The transition point is also the meeting point of the shock wave and the rarefaction wave reflected from the back wall of the tube. The situation is illustrated in Figure A1.1.

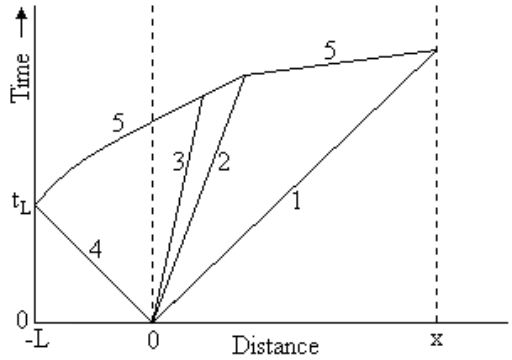

Fig. A1.1. Waves in a shock tube process.
1 = shock wave,
2 = interface of the system gas and the ambient gas,
3 = tail of the region where the pressure is constant,
4 = top of the induced rarefaction wave,
5 = top of the reflected rarefaction wave,
L = length of the pressurized part of the tube,
x = transition point,
t_L = arrival time of the induced rarefaction wave top into the back wall.

In the beginning of the shock tube process the propagated shock wave flows away from the cut point with constant pressure and velocity. At the same time the rarefaction wave is induced into the opposite direction. The top of the induced rarefaction wave reaches the end wall of the shock tube at the arrival time t_L:

$$t_L = \frac{L_s}{a_s} \tag{A1}$$

where
L_s = length of the pressurized part of the tube,
a_s = initial sound velocity.

After meeting the end wall the rarefaction wave reflects back toward the latter parts of itself. When the induced rarefaction wave has not yet met the reflected one, the wave is called to be in the simple state. After meeting the reflected wave it is called to be at the non-simple state [21].

The position x_{at}, where the gas having a sound velocity a exists at time t, can be obtained with the help of equation (2.4.1) as follows:

$$x_{at} = \left(\frac{2}{\kappa - 1} a_s - \frac{\kappa + 1}{\kappa - 1} a \right) t \tag{A2}$$

The differential equation of the position can be obtained as:

$$\frac{dx}{da} = -\frac{\kappa + 1}{\kappa - 1} t \tag{A3}$$

The velocity of the top of the reflected rarefaction wave is u_k:

$$u_k = w + a \tag{A4}$$

According to equation (2.3.2) and the one above we get the relative velocity:

$$u_k - u_a = 2a \tag{A5}$$

The relative change of the place of the top reflected wave at the time dt is:

$$dx = 2adt \tag{A6}$$

By substituting this equation into (A3) we obtain:

$$\frac{2adt}{da} = -\frac{\kappa+1}{\kappa-1}t \tag{A7}$$

By formulating, it follows that:

$$\frac{dt}{t} = -\frac{\kappa+1}{2(\kappa-1)}\frac{da}{a} \tag{A8}$$

By integrating equation (A8) we get the time t_{k1} when the top of the reflected rarefaction wave reaches the pressure of the shock wave:

$$\int_{tL}^{tk1}\frac{dt}{t} = -\frac{\kappa+1}{2(\kappa-1)}\int_{as}^{as1}\frac{da}{a} \tag{A9}$$

Here a_{s1} is the sound velocity of the system gas in the shock wave pressure p_1. At the moment the shock wave pressure stays constant. By solving equation (A9) we obtain:

$$\ln\frac{t_{k1}}{t_L} = \frac{\kappa+1}{2(\kappa-1)}\ln\frac{a_s}{a_{s1}} \tag{A10}$$

By formulating the above equation we get:

$$t_{k1} = t_L\left(\frac{a_s}{a_{s1}}\right)^{\frac{\kappa+1}{2(\kappa-1)}} \tag{A11}$$

The place where that happens is x_{s1}:

$$x_{s1} = (w_1 - a_{s1})t_{k1} \tag{A12}$$

The following important moment is t_1 when the top of the reflected wave reaches the interface of the system gas and of the ambient gas. This can be obtained from equation:

$$x_{s1} + (a_{s1} + w_1)(t_1 - t_{k1}) = w_1 t_1 \tag{A13}$$

By substituting equation (A12) into (A13) we get:

$$(w_1 - a_{s1})t_{k1} + (a_{s1} + w_1)(t_1 - t_{k1}) = w_1 t_1 \tag{A14}$$

By simplifying we get:

$$t_1 = 2t_{k1} \tag{A15}$$

The place w_1 where the top of the reflected rarefaction wave meets the interface is then:

$$x_1 = w_1 t_1 \tag{A16}$$

The moment, t_2, when the top of the reflected rarefaction wave meets the shock wave can be derived from:

$$w_1 t_1 + (a_1 + w_1)(t_2 - t_1) = u_1 t_2 \tag{A17}$$

Here a_1 is the sound velocity of the ambient gas in the shock wave and u_1 is the velocity of the shock wave. By solving the equation we get:

$$t_2 = \frac{a_1}{a_1 + w_1 - u_1} t_1 \tag{A18}$$

The transition point, x, where the reflected rarefaction wave meets the shock front can be determined as:

$$x = \frac{a_1 u_1}{a_1 + w_1 - u_1} t_1 \tag{A19}$$

By substituting equations (A1), (A11) and (A15) into (A19) we get:

$$\frac{x}{L_s} = \frac{2 a_1 u_1}{a_s (a_1 + w_1 - u_1)} \left(\frac{a_s}{a_{s1}} \right)^{\frac{\kappa_s + 1}{2(\kappa_s - 1)}} \tag{A20}$$

With the help of equation (2.4.7) we can get:

$$\frac{a_s}{a_{s1}} = \left\{ 1 - \frac{a_a / a_s (\kappa_s - 1)(p_1 - p_a)}{\sqrt{2\kappa p_a [(\kappa + 1) p_1 + (\kappa - 1) p_a]}} \right\}^{-1} \tag{A21}$$

By substituting equation (A21) into (A20) we get:

$$\frac{x}{L_s} = \frac{2 a_1 u_1}{a_s (a_1 + w_1 - u_1)} \left\{ 1 - \frac{a_a / a_s (\kappa_s - 1)(p_1 - p_a)}{\sqrt{2\kappa p_a [(\kappa + 1) p_1 + (\kappa - 1) p_a]}} \right\}^{\frac{-(\kappa_s + 1)}{2(\kappa_s - 1)}} \tag{A22}$$

With the help of the Rankine-Hugoniot equations, equation (A22) can be formulated as a function of the pressure p_1 as follows:

$$\frac{x}{L_s} = 2 \frac{a_a}{a_s} \sqrt{\frac{p_1}{p_a}} \frac{\sqrt{(\kappa + 1) p_1 + (\kappa - 1) p_a}}{\sqrt{2\kappa p_1} - \sqrt{(\kappa - 1) p_1 + (\kappa + 1) p_a}} \left\{ 1 - \frac{a_a}{a_s} \frac{(\kappa_s - 1)(p_1 - p_a)}{\sqrt{2\kappa p_a [(\kappa + 1) p_1 + (\kappa - 1) p_a]}} \right\}^{\frac{-(\kappa_s + 1)}{2(\kappa_s - 1)}} \tag{A23}$$

The transition distance ratio x/L_s depends on the shock wave pressure p_1, on the adiabatic factor of the system gas κ_s, and on the ratio of the sound velocity a_a/a_s. The transition distance ratio x/L_s as a function of the overpressure ratio p_1/p_a-1 is illustrated in Figure A1.2. It can be noticed that the transition distance is not constant.

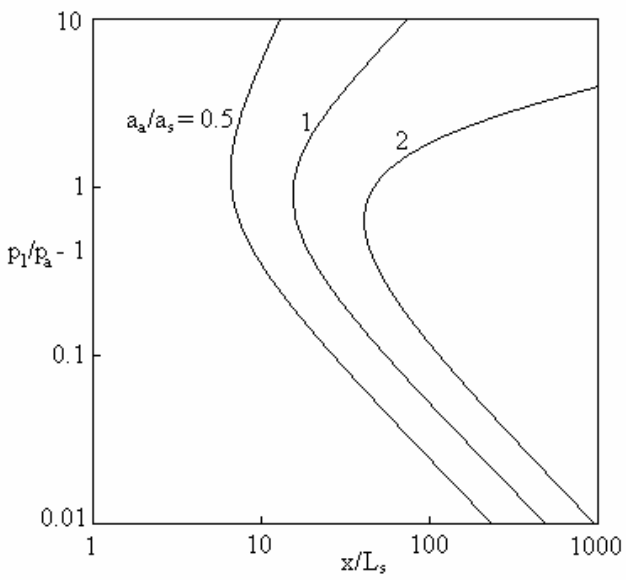

Fig. A1.2. Meeting point ratio x/L_s as a function of the relative starting pressure of the explo sion p_1/p_a-1 on different values of the sound velocity ratio a_a/a_s in a shock tube. The system gas and the ambient gas have a similar adiabatic factor $\kappa = 1.4$.

Next, the possibilities of the concept of isentropic exergy are examined. The isentropic exergy of a shock tube before the explosion process can be defined by the application of equation (2.1.7) as:

$$E = \frac{\kappa}{\kappa - 1} p_s A L_s \left[1 - \left(\frac{p_a}{p_s} \right)^{\frac{\kappa_s - 1}{\kappa_s}} \right] - A L_s \left(p_s - p_a \right) \qquad \text{(A24)}$$

where
p_s = pressure in the shock tube,
κ_s = adiabatic factor of the pressurized gas,
A = transverse area of the shock tube,
L_s = length of the pressurized part of the shock tube.

The loss of isentropic exergy at the simple state caused by the shock wave can be obtained by application of equation (2.3.16) as:

$$\Delta E = -\frac{\kappa}{\kappa - 1} p_a \left[\frac{(\kappa - 1)p_1 + (\kappa + 1)p_a}{(\kappa + 1)p_1 + (\kappa - 1)p_a} \cdot \left(\frac{p}{p_a} \right)^{\frac{1}{\kappa}} - 1 \right] Ax \qquad \text{(A25)}$$

where

ΔE = change of the isentropic exergy in the simple state,

p_1 = shock wave pressure,

x = transition distance.

The ratio of loss of the isentropic exergy in the simple state ε can be obtained from equation:

$$\varepsilon = \frac{-\Delta E}{E} \qquad \text{(A26)}$$

With the help of equations (A23), (A24), (A25) and (A26) the values of ε as a function of the overpressure ratio p/p_a-1 are illustrated below. The function is illustrated for two-atomic gases in Figure A1.3, for one-atomic gases in Figure A1.4 and for water steam in Fig A1.5. In the figures the functions are drawn with the values of sound velocity ratios of a_a/a_s = 0.5, 1 and 2.

In Figures A1.3, A1.4 and A1.5 it can be seen that in low overpressures of the shock waves the values of the loss ratio of isentropic exergy in the simple state ε are relatively constant. The ε-values seem to be 0.28…0.33.

This finding suggests that as the ε-value is quite constant in one-dimensional cases, it may be constant in the three-dimensional cases, as well.

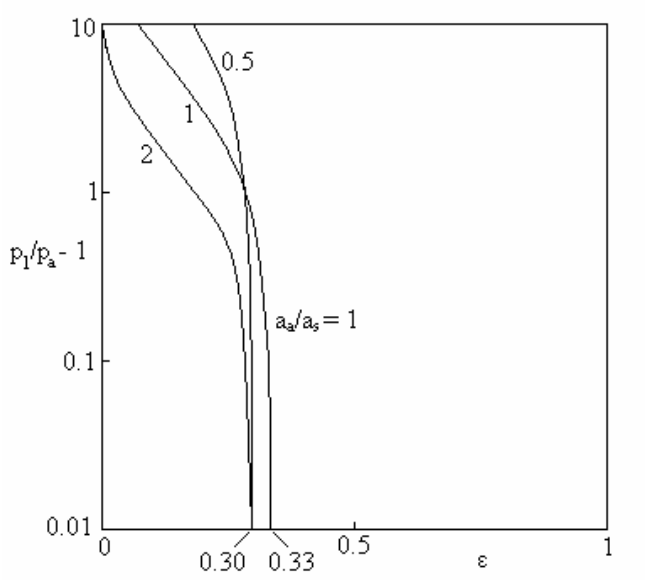

Fig. A1.3. Shock tube with air content. Shock wave pressure ratio $p_1/p_a - 1$ as functions of the loss ratio of isentropic exergy ε in the simple state by the transition point.
The system gas is two-atomic when $\kappa_s = 1.4$. The ambient gas is two-atomic when $\kappa = 1.4$.

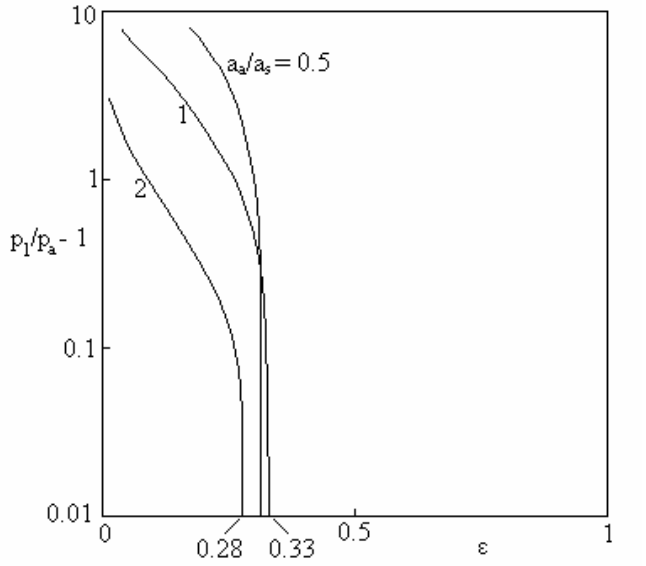

Fig. A1.4. The system gas is one-atomic when $\kappa_s = 1.667$. The ambient gas is two-atomic when $\kappa = 1.4$.

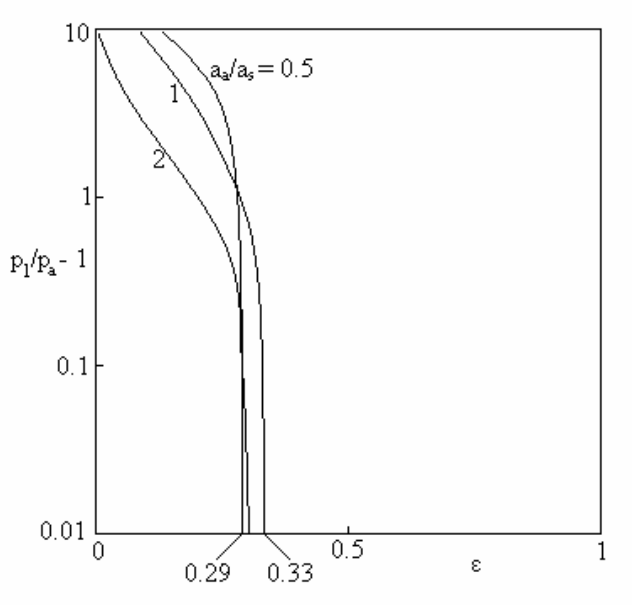

Fig. A1.5. The system gas is three-atomic (water steam) when $\kappa_s = 1.303$. The ambient gas is two-atomic when $\kappa = 1.4$.

Appendix 2

Table of the simple state

This table concerns the character of a hemispherically symmetric shock wave in the simple state. The symbols are:

p/p_a = relative pressure of the shock wave,

R_T = table distance,

E_T/p_a = cumulative loss of isentropic exergy per ambient pressure in the main shock wave.

p/p_a	R_T [m]	E_T/p_a [m^3]
101	1.000	-
91	1.142	12.93
81	1.325	33.08
71	1.567	66.05
61	1.902	124.14
51	2.391	236.6
41	3.163	485.2
36	3.736	726.2
31	4.528	1,144
29	4.934	1,396
27	5.410	1,725
25	5.975	2,163
23	6.656	2,763
21	7.490	3,603
20	7.980	4,150
19	8.531	4,814
18	9.154	5,627
17	9.864	6,633
16	10.68	7,894
15	11.62	9,497
14	12.73	11,570
13	14.04	14,290
12	15.62	17,930
11	17.54	22,950
10	19.94	30,030
9	22.99	40,420
8	27.02	56,270
7	32.52	81,850
6	40.45	126,100
5	52.74	210,700

p/p_a	R_T [m]	E_T/p_a [m^3]
4.5	61.76	281,700
4.0	74.04	390,800
3.8	80.28	450,200
3.6	87.54	522,800
3.4	96.11	612,800
32	106.3	726,000
3.0	118.8	870,600
2.9	126.0	957,800
2.8	134.1	1,058,000
2.7	143.2	1,173,000
2.6	153.5	1,307,000
2.5	165.3	1,463,000
2.4	178.9	1,646,000
2.3	194.6	1,864,000
2.2	213.1	2,125,000
2.1	235.1	2,441,000
2.0	261.7	2,829,000
1.9	294.5	3,312,000
1.8	335.8	3,924,000
1.7	389.3	4,717,000
1.6	461.3	5,771,000
1.5	562.8	7,226,000
1.4	716.3	9,338,000
1.35	826.5	10,710,000
1.30	974.0	12,440,000
1.28	1,048	13,240,000
1.26	1,133	14,120,000
1.24	1,233	15,120,000
1.22	1,351	16,250,000
1.20	1,493	17,530,000
1.19	1,575	18,230,000
1.18	1,666	18,980,000
1.17	1,769	19,800,000
1.16	1,884	20,680,000
1.15	2,014	21,630,000
1.14	2,163	22,670,000
1.13	2,335	23,800,000
1.12	2,536	25,060,000
1.11	2,773	26,440,000
1.10	3,058	28,000,000
1.09	3,407	29,760,000
1.08	3,842	31,770,000
1.07	4,403	34,120,000
1.06	5,150	36,890,000
1.05	6,197	40,300,000
1.04	7,767	44,640,000

p/p_a	R_T [m]	E_T/p_a [m^3]
1.035	8,889	47,170,000
1.030	10,380	50,130,000
1.028	11,130	51,430,000
1.026	12,000	52,850,000
1.024	13,000	54,360,000
1.022	14,190	56,030,000
1.020	15,620	57,870,000
1.019	16,450	58,860,000
1.018	17,360	59,890,000
1.017	18,390	60,990,000
1.016	19,550	62,170,000
1.015	20,860	63,420,000
1.014	22,350	64,760,000
1.013	24,080	66,210,000
1.012	26,090	67,770,000
1.011	28,470	69,480,000
1.010	31,330	71,360,000

ACTA UNIVERSITATIS LAPPEENRANTAENSIS

119. TAAVITSAINEN, VELI-MATTI. Strategies for combining soft and hard modelling in some physicochemical problems. 2001. U.s. Diss.

120. SAVOLAINEN, RAIJA. The use of branched ketene dimers in solving the solving the deposit problems related to the internal sizing of uncoated fine paper. 2001. U.s. Diss.

121. SARAVIRTA, ALI. Project success through effective decisions: case studies on project goal setting, success evaluation and managerial decision making. 2001. 286 s. Diss.

122. BLOMQVIST, KIRSIMARJA. Partnering in the dynamic environment: the role of trust in asymmetric technology partnership formation. 2002. 296 s., liitt. Diss.

123. KARVONEN, VESA. Development of fiber recovery process. 2002. U.s. Diss.

124. KÄYHKÖ, JARI. The influence of process conditions on the deresination efficiency in mechanical pulp washing. 2002. 87 s., liitt. Diss.

125. SAVOLAINEN, PEKKA. Modeling of non-isothermal vapor membrane separation with thermodynamic models and generalized mass transfer equations. 2002. 179 s. Diss.

126. KÄRKKÄINEN, HANNU. Customer need assessment: Challenges and tools for product innovation in business-to-business organizations. 2002. U.s. Diss.

127. HÄMÄLÄINEN, MARKKU. Spray coating technique as a surface treatment for woodcontaining paper grades. 2002. 121 s. Diss.

128. RANTA, TAPIO. Logging residues from regeneration fellings for biofuel production- a GIS-based availability and supply cost analysis. 2002. 182 s. Diss.

129. KUOSA, MAUNU. Numerical and experimental modelling of gas flow and heat transfer in the air gap of an electric machine. 2002. 97 s. Diss.

130. LAITINEN, NIINA. Development of a ceramic membrane filtration equipment and its applicability for different wastewaters. 2002. U.s. Diss.

131. SUNDQVIST, SANNA. Market orientation in the international context: Antecedents, consequences and applicability. 2002. U.s. Diss.

132. TORKKELI, MARKO, Technology selection and group decision support systems: Case studies on supporting strategic technology selection processes. 2002. U.s. Diss.

133. KYRKI, VILLE. Local and global feature extraction for invariant object recognition. 2002. 115 s. Diss.

134. HEIKKILÄ, TANJA. Permanent magnet synchronous motor for industrial inverter applications-analysis and design. 2002. 109 s. Diss.

135. HUTTUNEN, PENTTI. Data-parallel computation in parallel and distributed environments. 2002. U.s. Diss.

136. LIU, YONG. On sliding mode control of hydraulic servo systems and a manipulator. 2002. U.s. Diss.

137. JUHANTILA, OLLI-PEKKA. Establishing intercompany relationships: Motives and methods for successful collaborative engagement. 2002. 281 s. Diss.

138. PREIS, SERGEI. Practical applications of a systematic approach to the chemical abatement of pollutants in water and air. 2002. 234 s. Diss.

139. TIIHONEN, JARI. Influence of stationary phase and eluent properties on chromatographic separation of carbohydrates. 2002. U.s. Diss.

140. KILKKI, JUHA. Automated formulation of optimisation models for steel beam structures. 2002. 85 s., liitt. Diss.

141. LENSU, LASSE. Photoelectric properties of bacteriorhodopsin films for photosensing and information processing. 2002. 114 s. Diss.

142. KAURANNE, TUOMO. Introducing parallel computers into operational weather forecasting. 2002. U.s. Diss.

143. PUUMALAINEN, KAISU. Global diffusion of innovations in telecommunications: Effects of data aggregation and market environment. 2002. 153 s. Diss.

144. SARRETTE, CHRISTINE. Effect of noncondensable gases on circulation of primary coolant in nuclear power plants in abnormal situations. 2003. 114 s. Diss.

145. SAARENKETO, SAMI. Born globals – internationalization of small and medium-sized knowledge-intensive firms. 2002. 247 s. Diss.

146. IKONEN, KIRSI. Metal surface and subsurface inspection using nondestructive optical methods. 2002. U.s. Diss.

148. KOUVO, PETRI. Formation and control of trace metal emissions in co-firing of biomass, peat and wastes in fluidised bed combustors. 2003. U.s. Diss.

149. MOOSAVI, ALI. Transport properties of multi-phase composite materials. 2003. U.s. Diss.

150. SMOLANDER, KARI. On the role of architecture in systems development. 2003. U.s. Diss.

151. VERENICH, SVETLANA. Wet oxidation of concentrated wastewaters: process combination and reaction kinetic modeling. 2003. U.s. Diss.

152. STÅHLE, PIRJO, STÅHLE, STEN & PÖYHÖNEN, AINO. Analyzing dynamic intellectual capital: System-based theory and application. 2003. 191 s.

153. HAATAJA, JORMA. A comparative performance study of four-pole induction motors and synchronous reluctance motors in variable speed drives. 2003. 135 s. Diss.

154. KURRONEN, PANU. Torque vibration model of axial-flux surface-mounted permanent magnet synchronous machine. 2003. 123 s. Diss.

156. KUIVALAINEN, OLLI. Knowledge-based view of internationalisation – studies on small and medium-sized information and communication technology firms. 2003. U.s. Diss.

157. AHOLA, JERO. Applicability of power-line communications to data transfer of on-line condition monitoring of electrical drives. 2003. 141 s. Diss.

158. 1st Workshop on Applications of Wireless Communications. Edited by Jari Porras, Jouni Ikonen and Pekka Jäppinen. 2003. 67 s.

159. TUUTTI, VEIKKO. Ikkunoiden lasirakenteet ja niiden valintaan vaikuttavat tekijät. 2003. 294 s. Diss.

160. METSÄMUURONEN, SARI. Critical flux and fouling in ultrafiltration of proteins. 2003. U.s. Diss.

162. SORSA, TIA. The interaction of the calcium sensitiser levosimendan with cardiac troponin C. 2003. U.s. Diss.

163. KOVANEN, JANNE. Improving dynamic characteristics of open-loop controlled log crane. 2003. 97 s. Diss.